

"GENERATION OF WIND VELOCITY
FIELDS WITH SPECIAL REFERENCE
TO INTERPOLATION METHODS"

By

Peter L.W. Masibo

A Thesis submitted in partial fulfillment for
the degree of Master of Science in Mathematics
in the University of Nairobi.

October 1987

This thesis is my original work and has not been presented for a degree in any other University.

Signature: 

Peter L.W. Masibo

DEPARTMENT OF MATHEMATICS

UNIVERSITY OF NAIROBI

P.O. BOX 30197

NAIROBI, KENYA.

This thesis has been submitted for examination with our approval as University supervisors

Signature: 

Dr. W. Ogana

DEPARTMENT OF MATHEMATICS

UNIVERSITY OF NAIROBI

P.O. BOX 30197

NAIROBI, KENYA.

Signature: 

Dr. L. Ogallo

DEPARTMENT OF METEOROLOGY

UNIVERSITY OF NAIROBI

P.O. BOX 30197

NAIROBI, KENYA.

ACKNOWLEDGEMENTS

I wish to express my appreciation to the people without whose encouragement and assistance this study would not have been possible. My supervisors, Dr. B.W. Ogana and Dr. L.J. Ogallo, offered invaluable guidance during this study.

I owe special thanks to those people in the Kenya Meteorological Centre for enabling me to collect data. These include Mr. Okoola, and Mr. Mutulu. Also not forgetting Mr. Zach Mwangi of the Institute of Computer Science, University of Nairobi for assisting me with the enormous coding and programming on the computer.

I am grateful to Irene Karimi who helped in typing and general preparation of this work. I owe special thanks to Mr. Andrew Okeyo who went out of his way to advise me on the kind of data to collect and had a look at the method of analysis and made relevant changes.

I am indebted to the Faculty of Science and the University of Nairobi for awarding me the scholarship and the opportunity to pursue the M.Sc. degree.

Last, but by no means least, I wish to thank my parents without whose support, encouragement and insistence, I would not have come this far. -

(iv)

Dedicated to my parents who worked
unceasingly to educate me.

LIST OF FIGURES

<u>FIGURE</u>	<u>PAGE</u>
1. Kenya map showing the study area.	38
2. Wind Velocity Field for the season (December-February) at 13.00 hours.	41
3. Temperature Field for the season (December-February) at 13.00 hours.	42
4. Wind Velocity Field for the season (December-February) at 23.00 hours.	43
5. Temperature Field for the season (December-February) at 23.00 hours.	44
6. Mean flow by Streamline-Isotach Analysis for January season.	45
7. Wind Velocity Field for the season (March-May) and (September-November) at 13.00 hours.	48
8. Temperature Field for the season (March-May) and (September-November) at 13.00 hours.	49
9. Wind Velocity Field for the season (March-May) and (September-November) at 23.00 hours.	50
10. Mean flow by Streamline-Isotach Analysis for April season.	51
11. Mean flow by Streamline-Isotach Analysis for October season.	52

	<u>PAGE</u>
12. Wind Velocity Field for the season (June-August) at 13.00 hours.	54
13. Temperature Field for the season (June-August) at 13.00 hours.	55
14. Wind Velocity Field for the season (June-August) at 23.00 hours.	56
15. Temperature Field for the season (June-August) at 23.00 hours.	57
16. Mean flow by Streamline-Isotach Analysis for July season.	58

ABSTRACT

A two-dimensional objective analysis model was applied to a region near the equator. A vector field of surface wind velocities and a scalar field of temperatures were interpolated in the horizontal. The model provided an initial field by filling a computational domain of 320km by 240km divided into grids of 10km by 10km over an East-Coast area of Kenya. Terrain features were not incorporated in this model, since the region was largely of uniform topography.

The database for the study was from observations recorded by five stations within the area of study. Hourly values of velocities and temperatures were taken for the year (1983). The computed data sets were then grouped on a seasonal basis since there are seasonal variations of winds over the study area. The day (13 hrs) and night (23 hrs) records were however used to show diurnal variation of the wind field. The seasonal records were the fundamental database for the study.

The results from the study indicated that the interpolation scheme used gave reasonable wind and temperature fields for all the seasons, with the exception of the December-February season, compared with mean flow. The diurnal cycles of the wind and temperature fields were however reasonable during all seasons. It was also quite evident during all seasons that the land and sea breezes had significant impact on the wind characteristics over the study area.

Stronger coastal easterlies were observed in the afternoons during the March-May and September-October seasons when the effects of the sea breeze and synoptic scale winds are additive. The negative effects of the Katabatic winds at night over the eastern slopes were also quite evident during some seasons.

It is well known that some years have anomalous weather. The floods along the coastal region have been associated with stronger easterlies, while the coastal droughts have been associated with the weakening of the easterly wind or the development of westerly winds along the coast due to abnormal warming of the Indian Ocean. The year 1983 was dry along the coastal region. The deviation of the winds from normal which was observed during December-February season may therefore still be realistic.

TABLE OF CONTENTS

	<u>PAGE</u>
Title	(i)
Declaration	(ii)
Acknowledgement	(iii)
Dedication	(iv)
List of figures	(v)
Abstract	(vi)

CHAPTER 1

INTRODUCTION

1.1 Man and the winds	1
1.2 General flow	5
1.3 The atmospheric boundary layer	7
1.4 Objectives of study	9

CHAPTER 2

METHODS OF INTERPOLATING VECTOR AND SCALAR FIELDS

2.1 Introduction	10
2.2 Interpolation schemes	11
2.2.1 Least squares schemes	11
2.2.2 Optimum interpolation schemes	14
2.2.3 Weighted interpolation schemes	14
2.3 Kinematic methods	19
2.4 Dynamic methods	24

CHAPTER 3

APPLICATION OF INTERPOLATION METHODS

3.1 Introduction	28
3.2 Site of study	30
3.3 Method of analysis	31

CHAPTER 4

RESULTS AND DISCUSSION

	<u>PAGE</u>
4.1 Introduction	39
4.2 December-February season	39
4.3 March-May and September-November seasons	46
4.4 June-August season	52

CHAPTER 5

SUMMARY AND CONCLUSION	59
REFERENCES	61

CHAPTER 1

INTRODUCTION

1.1 Man and the Winds.

Since recorded history, wind energy conversion systems (WECS) have been employed to capture energy from the wind. There is evidence that wind energy was used to move boats on the Nile as early as 5000 B.C. and the simple wind mills were deployed in China for pumping water even earlier.

The world's appetite for energy is clearly on the increase in view of the continuing population expansion especially in third world countries. To satisfy this demand, additional energy production and research are required. Energy production from fuels is the source of environmental problems which do not seem to go away regardless of the progress in filtering and cleansing techniques. Hence, there is interest in renewable, non-polluting energy sources such as wind and solar energy, inspite of pessimistic cost benefit analyses.

Although wind purifies the air in some areas by dispersing germs, it is also a medium of transport for some pests and wind borne diseases together with atmospheric aerosols. Generally, wind has psychological as well as physiological influence on human beings since it is capable of effecting real microbial separations. Dust particles raised from the ground increase the microbial content of the atmosphere.

Man has always been obliged to protect himself from the severity of the wind and his first means of defence is undoubtedly to adapt his habitation to it. In his construction of dwellings, a careful outlook is given to shielding against possible droughts.

In normally moist conditions, if the ground is covered with vegetation, wind erosion is significantly reduced. Strong winds may still raise small quantities of soil and carry them from one place to another, thus contributing to formation of new soils. In areas where there are no trees and vegetation is limited to short grass, the deterioration of the vegetation cover may produce an extremely rapid acceleration of the process of wind erosion. Man has largely aggravated the dangerous effect of the climate by cultivating regions whose meteorological conditions are unsuitable for permanent cultivation, and by destroying the protective natural vegetation cover. Dust storms are particularly menacing during periods of drought or when hordes of insects have destroyed the vegetation and denuded the soil. Turbulence is another factor which lifts fine particles of dust by ascending currents. Temperature too has an important influence. A sudden change in direction of the wind, without any appreciable reduction of speed but accompanied by a large drop in temperature results in a marked increase of erosion. Soil erosion, in addition to the direct loss to agriculture raises several other problems.

It increases the cost of maintaining the railways, which have to be kept unencumbered. Roads also become buried and impassable and traffic accidents may occur as a result of thick dust.

The other effects of wind is in dehydration of plants. A steady wind accelerates transpiration, which increases the diffusion gradient from the stomata or pores to the surrounding atmosphere. Agitation of the leaves aggravates the process by causing air movement within the plant cells. In strong winds, bending of the leaf and alternate contraction and expansion of the tissues expel more moisture and leaves can die after a few days of vigorous shaking. Evaporization of water from the plant consumes heat and lowers the leaf temperature.

There are various wind systems formed around mountains and large water bodies that are important. Mountains hamper the wind, increasing turbulence and exerting frictional effects. Wind along valleys may therefore experience a high force. However, the general effect is to mitigate the full force of the wind as it proceeds. In so doing, mountains and hills bear the full brunt on their exposed slopes. It has been found that elevation affects the wind speed in that the deflected wind accelerates towards the top of windward slopes thereby increasing the wind speed at the crest. Wind increases in speed with

altitude, for instance, on a windy day the wind at sea level blows at roughly two thirds of the speed at 500 metres above sea level.

Large water bodies do exhibit their own wind systems. Thermal circulations which are closed are formed as follows: solar radiation heats the land mass causing a pressure drop because of the removal of air, this warm air is then replaced by cold air streaming in from the sea, which in turn becomes heated. The air above forms a return flow over the sea where it sinks and a closed circulation is established. The return flow takes place at 0.5-4km above the surface. The sea breeze convergence zone can result in air pollution problems and may cause thunderstorm activity in an unstable atmosphere. The inland penetration stops when the afternoon cooling destroys the maintenance of a pressure difference between the land and the sea. The strength and inland penetration of the sea breeze depend on atmospheric stability. Unstable planetary boundary layer can lead to a weak sea breeze circulation. The general direction of the ambient flow and the shape of the shoreline are important.

Local factors have significant influence on the weak regional winds especially at the lower and middle levels of the atmosphere. The differential heating between land and sea includes a flow which

often affects coastal areas. The local winds tend to modify the mean flow of air at the lower layers.

In the lowest areas of the surface layer, wind encounters small-scale obstacles which if grouped together form complex topography and result in complicated flow patterns. The obstacles frequently encountered are buildings, trees, groves, wind breaks, hills, valleys etc. Therefore, one finds that local wind shows considerable variations in strength and direction. The travelling weather systems or mesoscale circulation create a framework within which local factors determine the actual wind conditions.

1.2 General Flow

Since wind is air in motion, the potential energy of the atmosphere is therefore converted into kinetic energy through temperature and pressure gradients induced by the energy from the sun. Horizontal motion of winds in the atmosphere is important since it enables transportation of thermodynamic mechanisms while vertical motions are important in the production of clouds, precipitation and thunderstorms. The sun heats the air in the equatorial regions while the air at the poles is cooled by long-wave radiation. Differential heating of the surface of the earth and rotation of the earth are responsible for the large-scale motion systems that shape the general circulation of the atmosphere.

The mean flow of air over the earth is controlled by three general circulation cells namely the Hadley, Ferrel and Polar cells. The Hadley circulation transports the excess energy from the tropical region to the higher latitudes. The mean position of the Hadley circulation is between 0° - 30° latitudes. The tropical convergence zone (ITCZ) is the driving force in this circulation. Its mean position is situated around the equator but it migrates seasonally with the overhead sun. It pumps the hot humid air mass upto the middle latitudes and moves it toward the North and South of the two branches of the Hadley circulation. The Ferrel circulation which has a reverse pattern to the Hadley circulation is located in the middle latitudes (30° - 60°) while the flow patterns in the polar regions are controlled by the Polar cells.

The mean horizontal flow of the winds over the equatorial and polar regions are basically easterlies while westerlies dominate over middle latitudes. The winds over East Africa are therefore dominantly easterlies. The intensity and direction, however, vary significantly during the various seasons. The topographic pattern inland significantly modifies the basic flows. Typical gradient level speeds of equatorial easterly winds are of the order of 10 knots. (Atkinson, 1970).

Kidson et al (1969) on studying the intensity of the

easterly wind regime which characterizes the East African region found there were seasonal variations both in the zonal and meridional wind flow patterns. He observed that stronger tropical easterlies existed during the June-August period while weaker easterlies prevailed during December-February period.

During the December-February season, the north-easterlies dominate due to the strengthening of the Arabian and Azores high pressure cells. When the sun moves back to the equator, in March-May and September-November seasons, on-shore easterlies are quite intensive. During the June-August season, south-easterlies prevail due to the building up of the Mascarene and St. Helena anticyclones.

1.3 The atmospheric Boundary layer.

The environment in which WECS operate comprises the lower 1000 metres of the atmospheric boundary layer (ABL). It is therefore important to understand certain characteristics of wind flow within the ABL.

Many local factors affect the wind field and turbulence properties at a particular place. Buildings, groves and shelterbelts have a great influence on the local flow even if the effects die out rapidly downstream. In some cases, downstream effects can be felt 5-10km after passing over an obstacle. On flat

terrain, though, changes may occur due to surface roughness only. A change in roughness means that the boundary layer has to adjust itself to the new conditions by means of turbulent transfer of heat and momentum.

The upper boundary of the ABL is that part of the atmosphere where the effect of surface irregularities, or turbulence, disappears into the free atmosphere. The behaviour of the wind profile in the ABL due to frictional retardation on the surface of the earth is another important phenomenon. Over horizontally homogeneous surfaces, the logarithmic profile is used in neutral and stable conditions, but real wind variation with height usually deviates in the boundary layer and this restricts the vertical extrapolation to only where the vertical momentum flux is constant.

The Ekman layer is the layer between the surface layer and the top of the boundary layer where the shear stress term and heat flux go to zero. Ekman computed the solution of vertical current profile utilizing the components of geostrophic wind but real situations do deviate from the Ekman solution since it does not incorporate variables like baroclinity and non-stationarity. The Ekman

layer varies between the day-time convective, unstable boundary layer and the stable boundary layer at night-time. This is the reason for the geostrophic wind speed maximising during the night in higher latitude areas. These two types of the ABL are created due to the variational cooling and warming of the surface of the earth. The behaviour of the ABL has been studied and it had been found that the day-time turbulent exchange coefficients are much higher than the night-time coefficients. These studies also show that the diurnal variations of the ABL affect the wind velocity fields on the surface.

1.4 Objectives Of Study

1. To apply an interpolation scheme to generate surface wind velocity and temperature fields for a region in the East Coast of Kenya.
2. To interpret the resulting wind flow patterns and determine any characteristics due to seasonal variations.
3. To show understanding of the other methods of interpolation namely, the kinematic and dynamic methods.

CHAPTER 2

METHODS OF INTERPOLATING VECTOR AND SCALAR FIELDS

2.1 Introduction

Observational data taken by meteorological stations is never usually sufficient for all the purposes of weather prediction i.e. determination of building, determinations of the flow of pollutants in the atmosphere etc. Therefore interpolating methods have to be employed to generate data using the available data. Fields that are usually interpolated are wind, temperature and pressure. Interpolation of these fields could be either horizontal or vertical depending on the use. Horizontal interpolation is mainly done on the surface although the actually technique utilises the geostrophic wind in the free atmosphere where frictional effects are not felt. This kind of technique is suitable for the higher latitude areas and therefore does not apply in equatorial regions. Vertical interpolation is usually the power law.

The interpolation of some of the fields depends on the kind of field being interpolated for instance, in case of a vector field. This is due to the numerical non-uniqueness of a vector field.

Interpolation is normally done by what are known as objective analysis schemes, kinematic and dynamic methods as described further on,

2.2 Interpolation Schemes

Interpolation schemes especially of the class of objective analysis methods, do not solve the equations of the atmosphere to be able to generate data. They use the technique of curve fitting over irregularly spaced data to make it continuous.

In detail, discrete data can be made continuous by the use of several intrinsic factors for example, the use of historical information recorded about the area, the approach of some weighted average of the surrounding data values.

2.2.1 Least-Squares Schemes

The least-squares method is used to compute an approximate function on a set of discrete data. Assume values of a dependent variable y are given, often by measurement, for discrete values of the independent variable x , therefore we have specified values of $y(x)$ at $x = x_0, x_1, x_2, \dots, x_N$. We then seek an approximation $\bar{y}(x)$ to $y(x)$ such that the weighted sum of the squares of the errors (residuals) at these points is a minimum, that is:

$$S = \sum_{k=0}^N \left[W(x_k) \{y(x_k) - \bar{y}(x_k)\}^2 \right] = \text{minimum} \dots (2)$$

for some weights $w(x_k)$, $k = 0, 1, 2, 3, \dots, N$.

We look for an approximating function $\bar{y}_m(x)$ which has a number of parameters c_r ($r=0, 1, \dots, m$, with $m < N$).

For S to be minimum it requires that:

$$\frac{\partial S}{\partial c_r} = 0 \quad (r = 0, 1, \dots, m), \quad \dots \quad (3)$$

This, then, provides a set of algebraic equations which determine the parameters and they appear in a linear form as follows:-

$$\bar{y}_m(x) = c_0 \phi_0(x) + c_1 \phi_1(x) + \dots + c_m \phi_m(x), \quad \dots \quad (4)$$

where $\phi_0(x), \dots, \phi_m(x)$ are independent elements of a linear vector space of finite dimension $N+1$ functions on the set x_0, x_1, \dots, x_n , then the resulting algebraic equations, the normal equations, are also linear and given in a matrix form by

$$Ac = b. \quad \dots \quad (5)$$

Where c is the vector of parameters, A is a symmetric positive-definite matrix of order $m+1$, with elements independent of $y(x_k)$ and b is a vector depending on $y(x_k)$. In fact

$$a_{ij} = \sum_{k=0}^N w(x_k) \phi_i(x_k) \phi_j(x_k), \quad b_i = \sum_{k=0}^N w(x_k) \phi_i(x_k) y(x_k)$$

Following is a review of the objective analysis methods that have utilised the above formulation in their models.

Panofsky (1949) used a least squares method with a cubic polynomial fit over discrete data. The coefficients were determined by minimizing the sum of the squares of the difference between computed and observed values as in equation 2. At least ten sets of observation were required to solve the problem.

The difficulty with this scheme was that discontinuity occurred at boundaries of continuous areas which were fitted with different polynomials. The problem was subsequently solved by smoothing the resulting solutions and fitting quadratic surfaces at each grid point.

Generally, the problem with least squares fit is that ill-conditioning of the set of equations may occur and disruption of the whole system may result. Gilchrist et al (1954) developed an objective analysis method based on a two-dimensional second degree polynomial fit with subsequent interpolation for the height of the pressure surface at each grid point. Some precaution was necessary, for instance, when fitting a polynomial over a large area a smoothing technique had to be utilized. In minimizing, a weighting factor was introduced which was multiplied by the partial derivatives, from equation 3. This took care of random errors that arose due to assumptions like geostrophy in the vertical interpolation. A limitation of this model is that a grid point has to be surrounded by data stations and therefore a lot of data is needed.

McLain (1974, 1976) described a different polynomial fitting approach, in which the domain was triangulated, connecting the data points. A

second degree polynomial was then fitted to each value weighted according to its distance from a given triangle. The weighting used in the formulation had its radius of influence effectively set to the dimension of the region.

2.2.2 Optimum Interpolation Schemes.

These kind of interpolation methods are commonly used in initializing global or synoptic circulation models in meteorology. The interpolation function is formulated directly from past behaviour of wind (or temperature) field. This implies that a historical record of data values must be available in order to calculate statistical properties (Dartt, 1972). Moreover, these models are generally complex to implement (Gandin, 1963).

2.2.3 Weighted Interpolation Schemes

Cressman (1959) used pressure surfaces instead of wind vectors since pressure was more accurately measured. In the weighted interpolation method it is assumed that a grid value C_{ij} is some weighted average of the surrounding data value as follows:

$$C_{ij} = \frac{\sum_{k=1}^n C_k w_k(r)}{\sum_{k=1}^n w_k(r)} \dots (7)$$

Where C_k is the measured value of the scalar field at the k^{th} measuring station, $w_k(r)$ is the weighting function and r the distance from the grid point to the station.

In Cressman's method a weighting factor was used that was dependent on the distance of the station from the grid points. A correction term was included at each data station depending on the kind of observations. A smoothing function was incorporated for each four nearest grid points at the distance where the weighting factor rapidly approaches zero. The weighting factor that was used to aid interpolation in areas of irregularly spaced data was

$$W(r) = \frac{R^2 - r^2}{R^2 + r^2} \dots (8)$$

Where R is the distance at which the weighting factor goes to zero. Decreasing values of R were used on successive scans to analyze a spectrum of scans. The values obtained from each scan were then averaged to produce the final field. The method is applicable to an equatorial region if the geostrophic approximation is removed, especially in the vertical interpolation.

Endlich and Mancuso (1968) combined both polynomial fitting and distance weighting in their interpolation technique. A least squares fit to a first-order polynomial was performed using five of the nearest station values, according to

$$W(r) = \frac{a}{(r+r^*)^2 + a} \dots (9)$$

Where a is a constant, r the distance to the

station and r^* a distance factor ($0 \leq r^* < r$) that indicated whether the observation was an upwind-downwind ($r^*=r$) or crosswind ($r^*=0$) direction from the grid point.

A smoothing technique was employed since the polynomial could not fit the observations accurately. It had the feature of fitting an isolated observation closely but gave an average value of clustered observations especially in surface observations around cities. The model avoids oversmoothing and to make the analyzed grid point values agree more closely with the nearer stations a distance weighting, as described above, was included. This technique is good for areas with good data coverage, but gives erroneous results for places around the edges of the area due to other local effects.

Shepard (1968) discussed an interpolation technique in which a direction factor was included which accounted for shadowing of the influence of one data point by a nearer one in the same direction. The formulation of the weighting function included the effect of a barrier with a direction factor. If a "detour" of length $b(r)$, perpendicular to the line between the point (i,j) and the k^{th} measured station was required to travel around the barrier between two points, then $b(r)$ was considered to be the length of the barrier. An

effective distance r' was defined by

$$r' = \left[r^2 + b(r)^2 \right]^{\frac{1}{2}} \dots (10)$$

If no barrier separated the two points, then $b(r) = 0$.

Shenfeld and Boyer (1974) presented a technique for interpolation of a velocity field similar to that proposed by Endlich and Mancuso except that an exponential weighting factor was used in the distance weighting part.

McCracken and Sauter (1975) used an exponential weighting in their interpolation scheme of the form $w(r) = \exp(0.1)r^2$. This factor removed the complete dominance of a measurement near a grid point. Hovland (1977) in a pollution of air study computed wind and temperature fields using environmental data. This was an iterative procedure in which the radius of influence was decreased while the number of stations was increased on successive iterations. This was infact a modification of the Cressman's model. There was an advantage to this method such that the small-scale motions which are only detected in areas with dense

station data coverage were not spread to other neighbouring areas. The weighting function was similar to the Cressman function except that this was an exponential of the Cressman's weighting function.

Traci et al (1977) in their development of a Model called NOABL used an objective analysis scheme in their initialization. The technique was adopted with a weighting function of the form

$$W_k(r) = \frac{1}{r^2} \quad \dots \quad (11)$$

where $W_k(r)$ is the weighting factor and r_k is the distance away from the wind station. This method is similar to Shephard's since one could change the formulation to include the effect of barriers. Traci et al (1977) in the initialization scheme divided the atmosphere into two, the first was the upper layer which had a weighting function of the form

$$W_k(r) = \frac{1}{r} \quad \dots \quad (12)$$

and the second for the lower layers was as in Equation 11.

2.3 Kinematic Methods

Kinematic models generate a wind field from an initial field which is free from divergence. The models solve the some of the primitive equations and typically the continuity equations. Hence they are called mass-consistent algorithms.

The models utilize the principal of mass conservation (or continuity of mass) which can be used to deduce the vertical motion field from the knowledge of the horizontal velocity field.

The continuity equation in vector form is as follows

$$\frac{1}{\rho} \frac{\partial \rho}{\partial t} + \nabla \cdot \vec{v} = 0 \quad \dots \quad (13)$$

where ρ is the density of the fluid and \vec{v} is the vector dimension of the velocity u, v, w along the cartesian axes x, y, z .

Here, the flow is frictionless and irrotational and hence is known as potential flow which implies that velocity is derived from a scalar velocity potential ϕ such that

$$\vec{v} = -\nabla \phi \quad \dots \quad (14)$$

and therefore treating an incompressible two-dimensional potential flow. We define vorticity since the flow is irrotational by

$$\text{curl } \vec{v} = 0 \quad \dots \quad (15)$$

In vector form the velocity potential can be used in conjunction with equation 15 to derive the

velocity components of the form

$$u = -\partial\phi/\partial x, \quad v = \partial\phi/\partial y \quad \text{which if substituted}$$

in the incompressible form of the continuity equation

$$\nabla \cdot \vec{v} = 0 \quad \dots \quad (16)$$

therefore, for a two-dimensional steady incompressible potential flow, $\nabla^2\phi = 0$. \dots (17)

The following is a survey of the kinematic models and their implementation of the continuity equation.

Sasaki (1958, 1970 a,b) developed a variational analysis technique which defined a function that was to minimize the variance of the difference between the observed and analyzed variable values subject to certain constraints which were satisfied exactly or approximately by the analyzed values. In this formulation the continuity equation was equated to a residual error, ϵ such that

$$\frac{\partial h_o}{\partial t} + \frac{\partial(u_o h_o)}{\partial x} + \frac{\partial(v_o h_o)}{\partial y} = \epsilon \quad \dots \quad (18)$$

where u, v, h are observed values and h is the height of the inversion base above the topography, u, v are the x and y velocity components. Sasaki's model equates the residual error to a lagrangian multiplier λ such that $\nabla^2 \lambda = \epsilon$. \dots (19)

As one can see, λ takes the form of a velocity potential.

Dickerson (1973) in his model applied equation

18 with the Euler-Lagrange equations with both strong constraints which means that ϵ has to be exactly zero and the weak constraints meaning that ϵ could be approximately reduced to zero. The use of the continuity equation was to produce a divergence free wind field.

Liu et al (1976) modified Dickerson's model by using an iterative algorithm on equation 18 while ignoring $\frac{\partial h}{\partial t}$ since it was very small compared to the other terms. These results were compared with a fixed-vorticity scheme in which the same initial wind field was input. The fixed-vorticity scheme is usually related by an elliptical differential equation obtained from a stream function $\psi(x,y,t)$ and vorticity $\zeta(x,y,t)$ such that

$$\nabla^2 \psi = -\zeta. \quad \dots \quad (20)$$

An error of about 25% of the initial wind field to the observed data was observed. In the tropics divergent wind field is equally strong compared to non-divergent wind field (Kavishe, 1983).

Traci et al (1977) developed a model using an initialization scheme to fill up the computational mesh. The vertical component was interpolated by a power law and the resultant wind fields were corrected using perturbation velocity potential and transmissivities. Then the divergence was minimized by solving the continuity equation in three

dimensions. The coordinate system was changed to sigma coordinates. The solution was by line-over-relaxation iteration. This model advances a suggestion that the correction does not remove initial vorticity in the wind field data.

Sherman (1978) developed a variational objective analysis model which was used to predict transport in the atmosphere. Mass-consistent input fields were used to determine wind fields over complex terrain. Basically, a function was found and by using the Euler-Lagrange equations and the continuity equation, the residual error was minimized according to strong constraints. The numerical technique of solution was by central differencing scheme. The condition on the boundaries that there be no flow was incorporated since it is the basis of all kinematic models. Limitations were found to be around barriers and therefore adjustment were made to allow flow around the barriers. It is a good diagnostic model for calculating mean wind fields for transport and diffusion problems.

Bhumralker et al (1980) modified Sherman's model by incorporating terrain-following coordinates and the initialization process for this model was by the objective analysis technique by Endlich et al (1968). The numerical technique was by a relaxation method.

Endlich et al (1982) modified Bhumralker's model by incorporating the logarithmic profile for the vertical component field to the geostrophic height. Though the method improved the results, it is not applicable to the tropics since as one approaches the equator the coriolis term disappears rendering the geostrophic equations useless. Therefore, vertical interpolation is not possible. Also to be able to use the logarithmic profile, the planetary boundary layer must be neutral. A suggestion would be the modification of the power law to use in different states of the planetary boundary layer.

Lalas (1986) modified the model by Traci et al (1977) by incorporating a logarithmic profile for the vertical component but basically solved similar equations.

Davis et al (1984) developed two different codes ATMOS1 and ATMOS2. The model incorporates the conformal coordinates with a hydrostatic approximation. The diagnostic wind field (ATMOS1) was a variational technique which solved Sherman's equations and the method of solution was by successive-over-relaxation. The advection diffusion code (ATMOS2) utilized the sigma coordinates and solved the concentration equation by an implicit scheme for diffusion.

2.4 Dynamic Methods

Dynamic models that have been developed solve most or all the primitive equations with sophisticated turbulence closure schemes. Dynamic models are difficult and expensive to implement, since they include many parameters (Lalas, 1985). However they more accurately forecast many meteorological variables than can be done by kinematic models.

The basic primitive equations solved in these models are the two prognostic equations namely, the x and y components of the momentum equation and the thermodynamic energy equation and the three diagnostic equations namely, the continuity equation the hydrostatic approximation and the equation of state.

Most models do solve a modified form of the primitive equations as given by Haltiner (1971). Thus assuming the hydrostatic approximation to hold these equations are as follows

$$\frac{\partial \rho}{\partial t} + \nabla_H \cdot (\rho \vec{v}_H) + \frac{\partial}{\partial z}(\rho w) = 0 \quad \dots \quad (21)$$

$$\frac{D\vec{v}_H}{Dt} = -fkx \vec{v}_H - \frac{1}{\rho} \nabla_H P + \frac{1}{\rho} \frac{\partial \vec{\tau}}{\partial z} + \vec{F}_{\theta H} \quad \dots \quad (22)$$

$$\frac{\partial P}{\partial z} = -\rho g \quad \dots \quad (23)$$

$$\frac{De}{Dt} = - \frac{\theta}{PC_p T} \frac{\partial F_{\theta v}}{\partial z} + F_{\theta H} \quad \dots \quad (24)$$

Where ρ , p , θ are density, pressure and potential temperature respectively, coupled by the equation of state, \vec{V}_H is the horizontal wind speed, w the vertical component of the wind velocity, $\vec{\tau}$ the Reynolds stress tensor, F_{MH} and $F_{\theta H}$ the horizontal diffusion of momentum and heat and $F_{\theta V}$ the vertical flux of sensible heat. The gradient ∇_H has derivatives only in the horizontal directions.

These equations have been modified to appropriately to apply in the atmosphere. Here follows a review of the models that utilized the above equations in their solutions of the hydrodynamic equations.

Mahrer and Pielke (1977) developed a three dimensional model which solved the primitive equations of mass, momentum, energy with a closure scheme based on the parametrization of the k-theory by Businger (1971). The model was developed to simulate sea breeze circulation to obtain three-dimensional mesoscale wind fields. In addition, boundary conditions on the ground were modelled differently using the temperature equation. The solution was found by forward-in-time, semi-implicit and upstream differencing of the advective terms with cubic spline. The kind of data that was required for this simulation was elevation and ground properties (albedo, conductivity or temperature). Finally, the transport coefficients required a closure scheme.

Patnaik (1979) developed a three-dimensional model that solved the primitive equations

for wind velocity, potential temperature and moisture including effects of advection, stratification, coriolis force, turbulent fluxes of momentum, heat, moisture and radiation. It utilized terrain-following coordinates based on hydrostatic approximation. Solution was by time integration based on the leap frog scheme.

Other people who developed models that required the solution of the primitive equations with hydrostatic approximation accompanied by sophisticated closure schemes were Seaman and Anthes (1981). Lee et al (1982), Yamada (1983) and Garrett (1983, 1984).

All dynamic models require the use of a turbulent closure scheme. The turbulent scheme are mostly derived from turbulent fluctuations or deviations from the mean so that a dissipative system contains a certain amount of energy. Usually energy is the basis of turbulent motion and it is called turbulent energy.

There is no explicit method that is best all round especially for steady state solutions since the night-time boundary layer and the transition periods are not fully understood. They also may require the solution of a number of non-linear partial differential equations which in turn require a large amount of boundary values that

are difficult to obtain. This makes their use computationally expensive and thus uneconomical in both financial cost and human resources required.

CHAPTER 3

APPLICATION OF INTERPOLATION METHODS

3.1 Introduction

In this study an interpolation scheme was applied to an East Coast area of Kenya. The generation of wind velocity and temperature fields was necessary so that wind and temperature patterns could be monitored closely for this particular area. Moreover the patterns also can show thermal circulation formed due to the different heating of the surfaces. These circulations which are formed are instrumental in weather prediction. This is an important aspect since variation of the rainfall in Kenya is closely associated with the large scale flow of wind intertwined with the inland flow effect of the sea breeze. These diurnal characteristics of the land/sea breezes are sometimes additive to the large scale flow of the winds in some seasons. This is, infact, the reason for short and long rains in Kenya. Also, one can be able to determine the dry, wet and normal years in Kenya after carefully studying the wind patterns of generated fields for a large area.

Interpolation schemes are used in this study since they are easier to implement. The higher-order methods namely, the kinematic and dynamic models are expensive to implement, though, they can furnish one with more reliable patterns than the interpolation methods.

Further, the kinematic and dynamic models that have been developed, have only been implemented in higher areas. Therefore, modification has to be done to utilize them in equatorial regions. In the horizontal interpolation of this models, they utilize the idea of geostrophic wind in upper layer, but as one approaches the equator, the coriolis factor disappears and therefore the geostrophic equation no longer holds. Lastly the time involved in the implementation is another disadvantage of these models.

The interpolation that was implemented in this study is by Traci et al (1977). This method utilized the approach of interpolation of irregularly spaced data onto a regular grid drawn within the study region and assumes that a grid value, C_{ij} , is some weighted average of the surrounding data values.

$$C_{ij} = \frac{\sum_{k=1}^n C_k W_k(r)}{\sum_{k=1}^n W_k(r)} \quad \dots \quad (25)$$

where C_k is the measured value at the k^{th} measuring station, $W_k(r)$ is the weighting function and r the distance from the grid point to the station. The averaging technique which was adopted had a weighting function of the form

$$W_k(r) = \frac{1}{r_k^2} \quad \dots \quad (26)$$

where $W_k(r)$ is the weighting factor and r_k is the distance away from the wind station. No barriers were incorporated in this model since the study area is

largely of flat terrain. Surface roughness, due to a change from the sea to land, was not considered in this study. Usually surface roughness plays a major role in vertical interpolation. Also, surface roughness has a stronger effect in unevenly changing terrain. This interpolation scheme was preferred more than the exponential and cubic spline methods because of its simple formulation. As by Traci et al (1977), the interpolation scheme could be changed to fit for different layers, for example the lower layers of the atmosphere a weighting function of the form of equation 26 given here in more detail as

$$W_k(r) = 1/r_k^2 \quad \dots \quad (27)$$

where r_k is the distance away from the wind station; for this case $r_k^2 = x_k^2 + y_k^2$, x , y are the axes of the computational domain and k is the number of wind stations in domain, while for the upper layer a function of the form that

$$W_k(r) = 1/r_k \quad \dots \quad (28)$$

was adopted. In this study the formulation for the lower layers was adopted since the generation of the data was on the surface (820mb).

3.2 Site Of Study

The area of study lies south of the equator enclosed by latitudes $1\frac{1}{2}^{\circ}\text{S} - 5^{\circ}\text{S}$ and by longitudes $37^{\circ}\text{E} - 40^{\circ}\text{E}$ and has an area of 76,800 sq. km. It is dominantly a costal lowland which slants towards

the boundary of the Kenyan coast and the Indian Ocean closely following the shape of the Kenyan coast from south of Mombasa towards Lamu. Inland of this area the Tsavo Park and Machakos district areas are covered. The area widens towards Garissa but does not enclose the Garissa meteorological station.

Plains and hills loom within the area. Towards the coast, the area slopes down gently from a height of 3000 metres near the slopes of Mt. Kenya to sea level covering a distance of about 400km. The vegetation cover is a mantle of small trees of bushy habitat together with lesser bushes and shrubs. This vegetation is evergreen or partially green. The general level of the mantle is between 5m and 10m, while grass cover is generally below savannah level, commonly thin with mainly basal foliage and various animal species. Along the coast the vegetation is woodland and is an evergreen type of vegetation. Closer to the ocean the natural vegetation is mainly mangrove since mangroves grow in tidal swamps unsuitable for human settlement. The study domain is given in fig. 3.1.

3.3 Method of Analysis

The raw data was acquired from Kenya Meteorological Centre. The data is collected in hourly, daily and monthly groups, and recorded down in the registers of reports; the "meter" and "speci" code books. This information is collected manually from the various stations all over the country. The stations are not close, they are approximately 100km away from each other and some places

even further away. The data differed as some of the data was collected by anemometers and wind vanes. The anemometer which is located at Mombasa airport is 10m high while the other stations inland, which are wind vanes, are located at 2m high. Since the land rises gently from the coast no correction was used to fit the values to a particular height before the computations.

The surface wind velocity and temperature fields were collected for five stations spanning over a full year at hourly intervals i.e. Mombasa airport, Voi, Makindu, Malindi and Lamu. These data source was limited to one year due to lack of time and the cost factor of collecting and coding was escalating. The stations were based within the study region in which a computational mesh was formed. The region covered land area of 76,800 sq. km. when compounded. Grid points were of the size 100 sq. km. culminating to 768 stations within the computational domain.

The data set consisted of only five stations which were then interpolated for remaining grid points. In this view the data set was irregularly spaced. To maximise data availability, hourly values were preferred to synoptic values.

The computational domain was rectangular such that the use of the axes would be incorporated. The x-axis coincided with one side of the rectangle from the coast proceeding inland of the domain, while the y-axis coincided with alternating side of the rectangle

along the coastline. A lot of care was taken such that four of the stations coincided with a grid point within the mesh. This made it easier to calculate the distance of the station from any of the grid point or from another station. The data value at the station was not recalculated but the original value from the data set was kept when computation was at the grid point of the particular station. Therefore, the original values at the respective grid point, which was coincident with the station, were printed in the final generated field. Due to these massive data set and small computer memory, a method was designed to keep each month's data in different computer files. This created was a total of 12 files for wind speeds and direction and another 12 files for the temperature field.

Mean hourly wind fields were computed on the raw data by resolving to get the easterly and westerly components separately. The components in one direction were added and averaged depending on the particular season. This made it easier to separate the stronger easterly winds from the weaker westerlies. It was done by the help of the rule that the zonal component is positive when directed eastwards and negative when directed westwards.

The following formulae was used, zonal (u) and meridional (v)

$$u = - |\vec{v}| \sin \phi$$

$$v = - |\vec{v}| \cos \theta$$

where \vec{v} is the individual observed wind speed to the station, ϕ is the observed wind direction measured from the true North of the compass. The procedure was repeated for all the months in each season, bearing in mind that some months exhibit the same kind of flow i.e. March-May (long rains) and September-November (short rains) which have an dominantly easterly flow. The essence of dealing with the components was therefore in close agreement with the background flow. These mean seasonal values were also kept in different files in the computer for subsequent computation.

The temperature (scalar field) was treated similarly when fitting the data into the computational domain. The generation of data into the mesh was by the same method as in the wind field. This was necessary to monitor the changes of the wind speed and direction due to temperature variation. Basically effects of thermally driven winds of the lower atmosphere would be monitored.

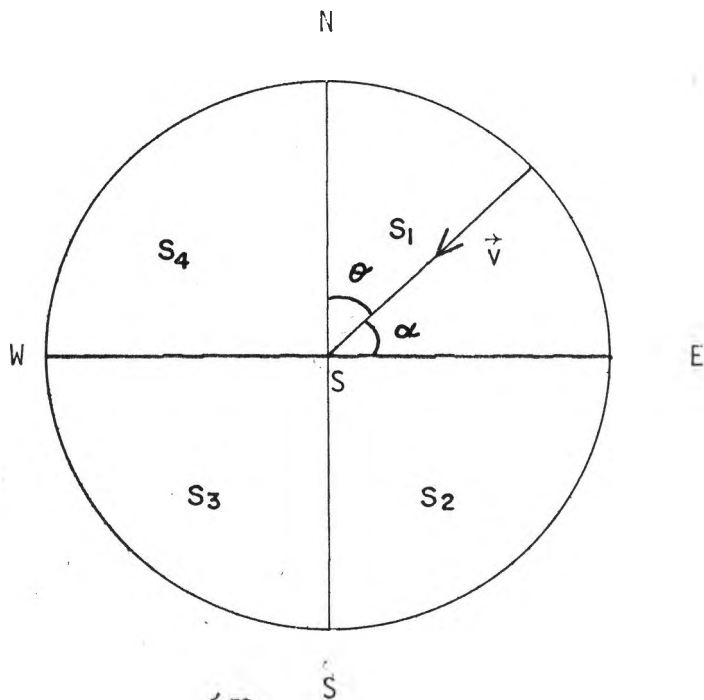
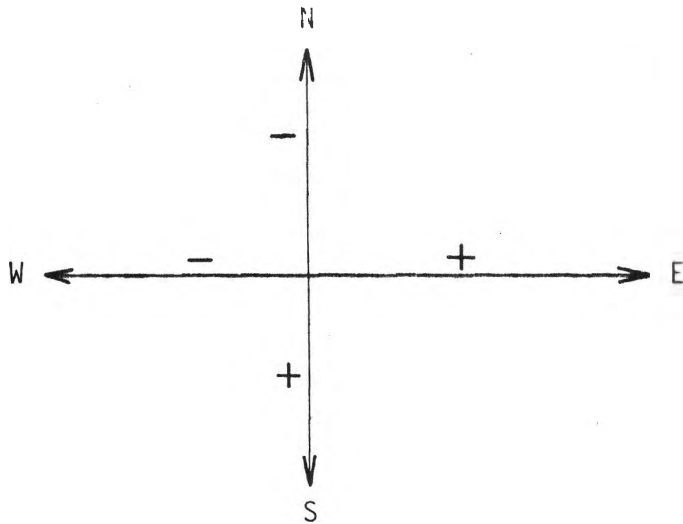
A computer program was then written to interpolate data to each of the grid points. Since there

were 24 files in total, seventy two runs of the program on the different files was sufficient to produce the final numeric fields.

In case of the vector field (wind field) the approach varied in the sense that, the directions for every grid point had to be recalculated by the use of the pythagorous theorem from the components but the final wind speed was calculated from the mean magnitude value. The paper by Schaffer et al (1979) on the numerical non-uniqueness of a vector field interpolation, shows that the use of components to inpterpolate for the wind speed does not yield the same results as the use of magnitudes to interpolate for wind speed (scalar field). An error is added on the original value.

Due to the small memory and not up-to-date computer operating system, the decision to use small files in which to do the various computations was advantageous. The long hours of running programs were dispelled. Also it was convenient for one to run the programs when job scheduling was low within the computer, especially when the users were not many.

The following diagram was used in the recalculation of directions from the zonal and meridional components.



θ , the angle from the true North and consider the quadrants as S_1 , S_2 , S_3 and S_4 , α is the angle subtended by the vector \vec{v} from the East-West direction where \vec{v} comes into the station, S.

The generated results for directions were in components represented by u' for the Easterly and Westerly component, while v' was for the Northerly and Southerly components. Therefore the direction was then recalculated depending on the sign of the component as follows,

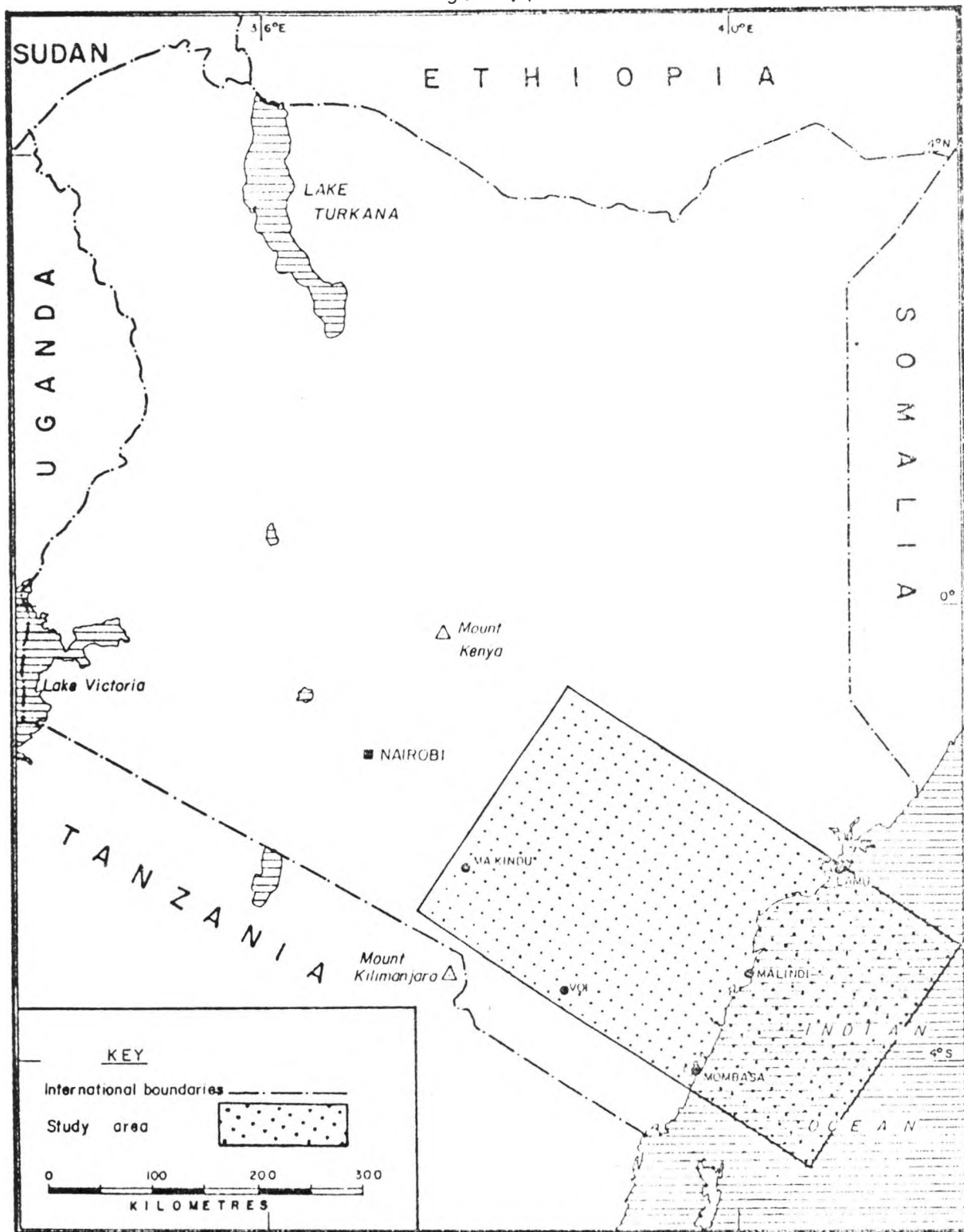
$$S_1 \text{ Quadrant, } \theta = 90 - \tan\left(\frac{v'}{u'}\right)$$

$$S_2 \text{ Quadrant, } \theta = 90 + \tan\left(\frac{v'}{u'}\right)$$

$$S_3 \text{ Quadrant, } \theta = 270 - \tan\left(\frac{v'}{u'}\right)$$

$$S_4 \text{ Quadrant, } \theta = 270 + \tan\left(\frac{v'}{u'}\right)$$

fig. 3.1



WIND VELOCITY AND TEMPERATURE
FIELDS OF COASTAL AREA OF KENYA

CHAPTER 4

RESULTS AND DISCUSSION

4.1 Introduction

The results generated were of wind speeds and corresponding directions and temperature fields. These results were generated numerically but due to massive data, only certain values were made out into charts and presented. The presented results were ^{the} inform of wind velocity and temperature field charts for particular times of the day and night. This was necessary to show the diurnal characteristics of the temperature and wind field. It is also possible, therefore, to see thermally driven winds, since the study area was basically situated near a large water mass and land.

It was necessary to subdivide the charts further according to the four basic seasons namely December-February, March-May, June-August and September-November season. The season March-May corresponding to the long rains and the September-November to the short rains were combined in this study since they exhibit the same kind of easterly flow.

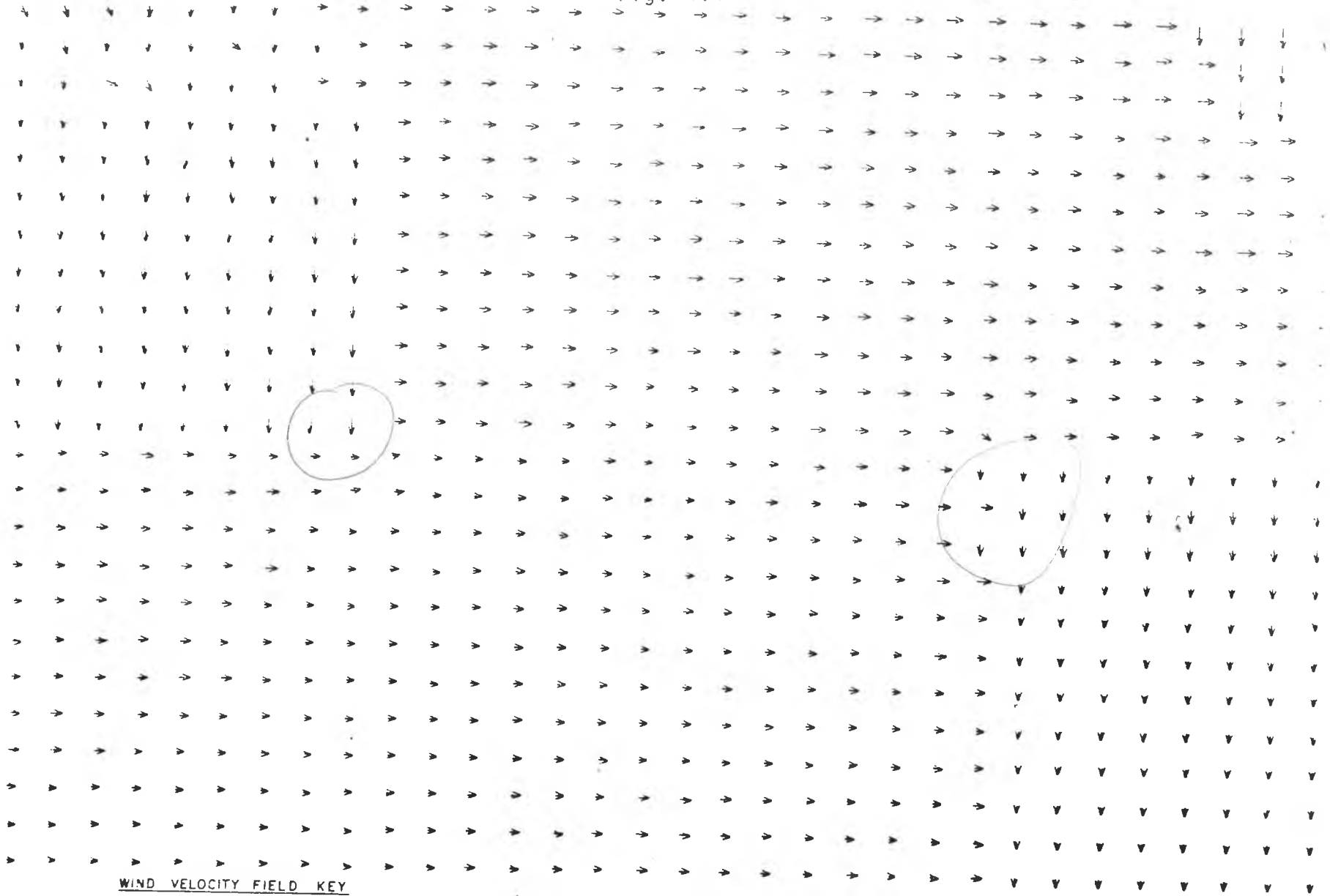
4.2 December-February Season.

The mean flow in this season is basically north-easterlies as given by figure 4.5 from Findlater (1968) at 850 mb. From our study the night time wind velocity for this season is given in figure 4.1 and the temperature field in figure 4.2. The map of

the site of study (Figure 3.1) shows that the North - Eastern section is within the sea, and shows a northerly wind blowing towards Malindi, but after 30km of travel, the wind changes and starts becoming westerly. This is probably due to obstruction by a land mass around Lamu. The wind blow in a westerly manner and then changes again to a northerly in the South-East sector. The wind speed is however reduced. From the South-West sector, the wind steadily blows in a westerly direction. This is perhaps due to the katabatic flow formed as a result of the eastern-slopes of Mt. Kenya which is outside the study area but whose effects are felt in this flow. This trend of flow is disrupted further south of the chart due to the Mt. Kilimanjaro slopes. The wind speed by this time has reduced to about 1 m/s, but blowing now in a westerly direction. In this study, the katabatic winds are very instrumental in the production of westerly flows accompanied by low wind speeds especially at night time.

On the corresponding temperature chart, the sea is at a higher temperature than the land. The temperature variation is almost 1°C in every 60km from the sea to land. As noticed the temperature decreases inland to about 19°C in the North-West sector. The formation of a land breeze is therefore evident, due to the difference in the heating of the land and ocean surfaces.

fig. 4.1



WIND VELOCITY FIELD KEY

23 00 HRS

WIND VELOCITY FIELD KEY
13 00 HRS

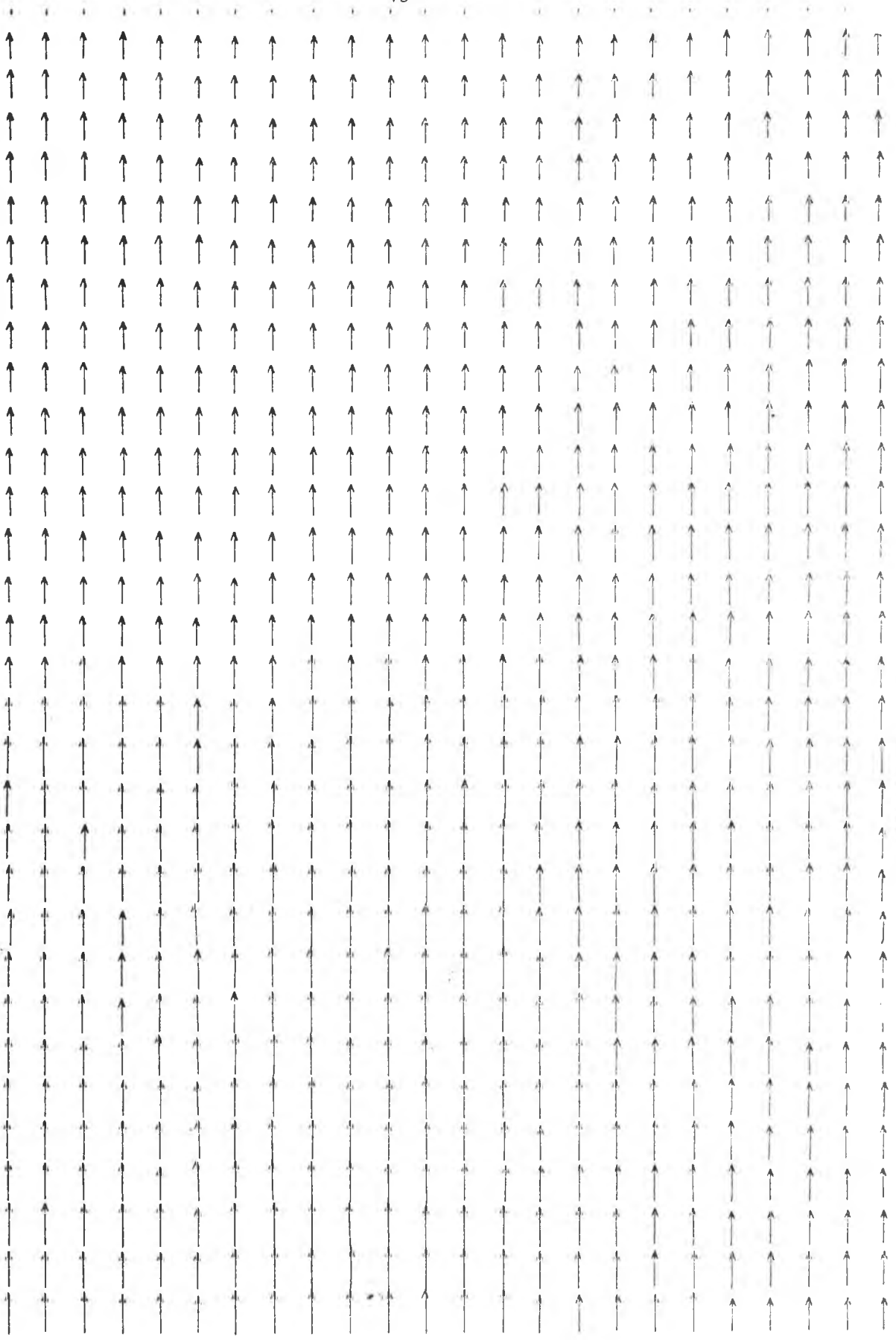


fig. 4.3

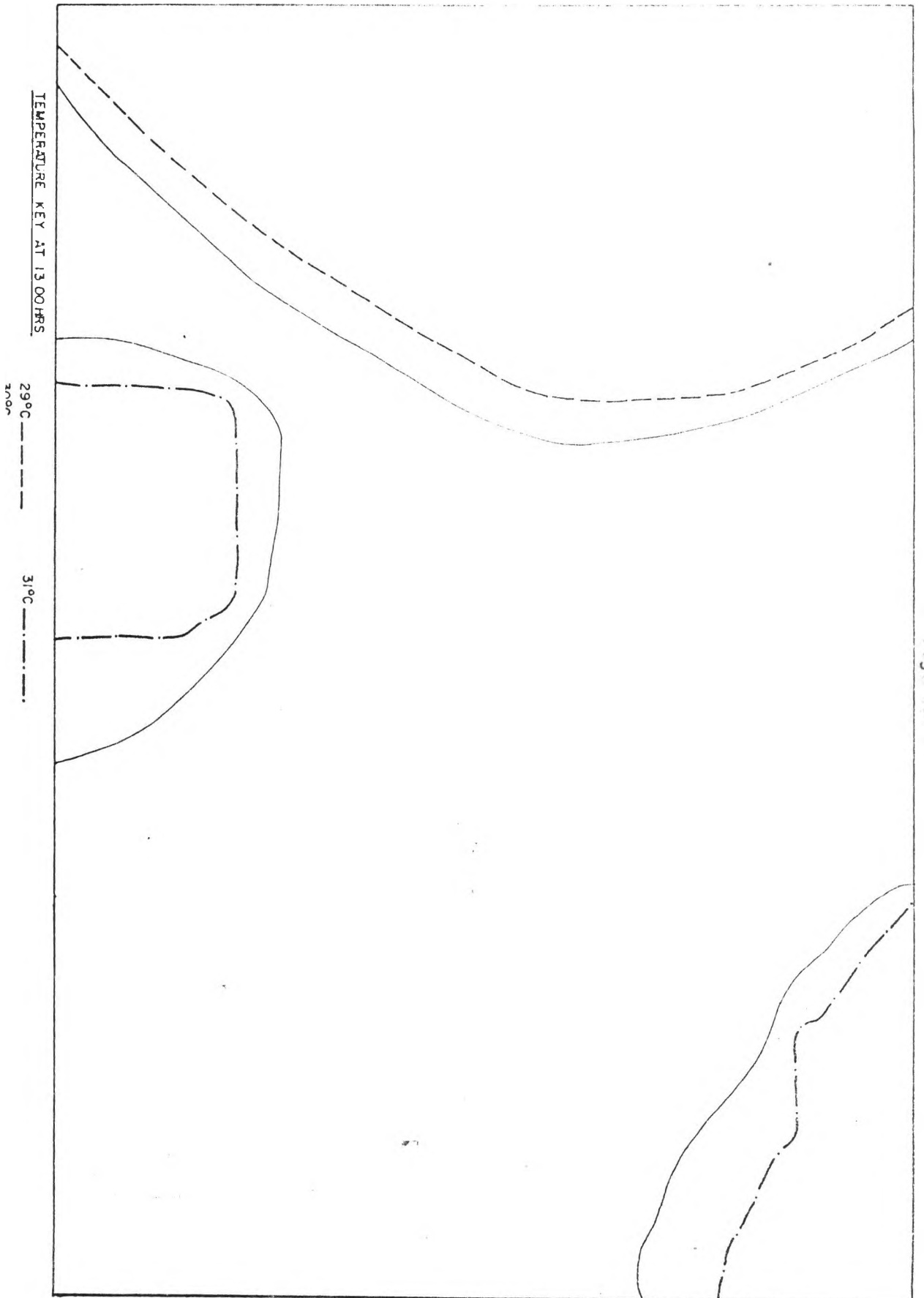
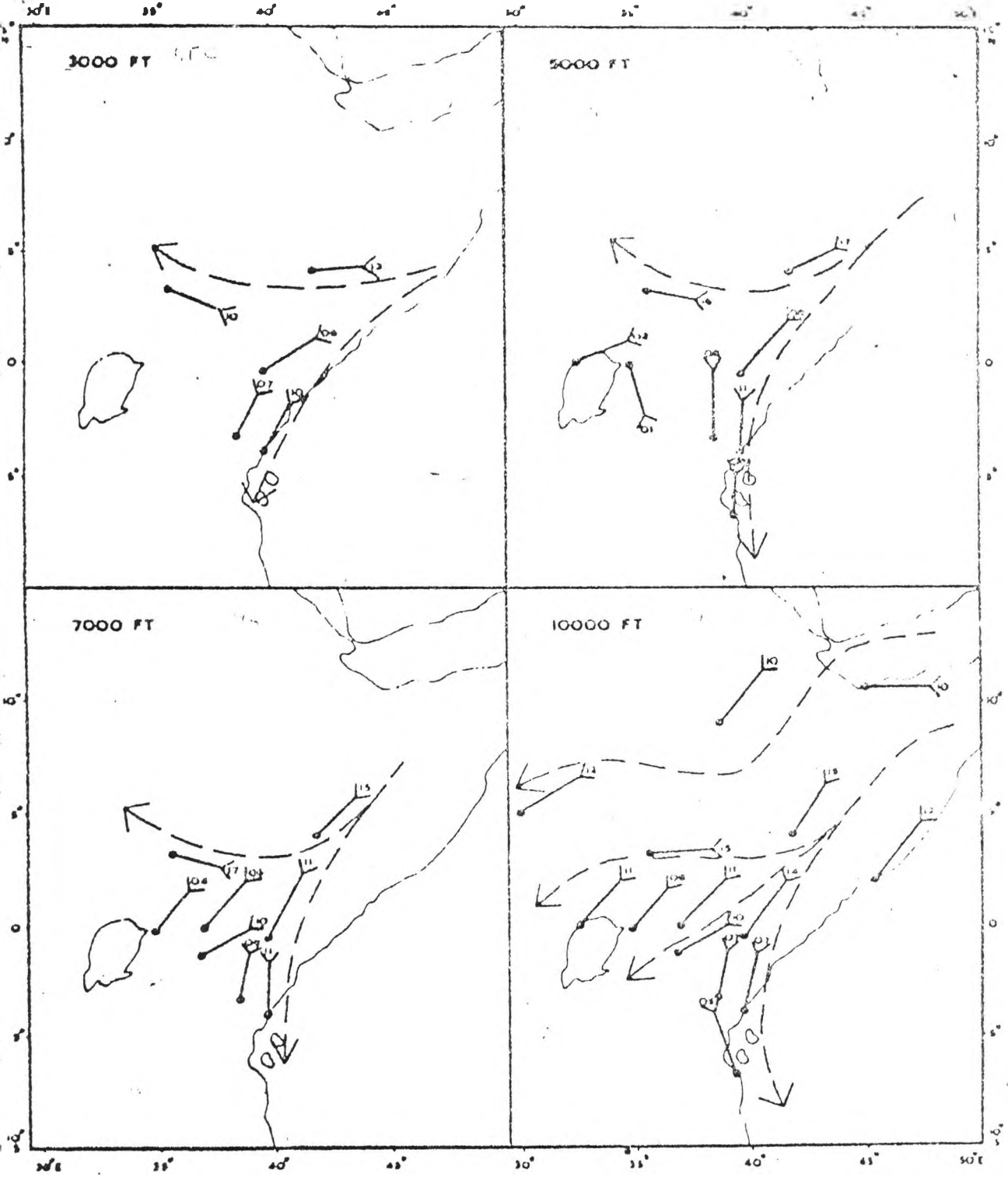


fig. 4.4

fig. 4.5

JANUARY



Both charts represent conditions at about 23 hours when land is cooler than the sea. Minimum and maximum temperatures at this time are 19°C and 26°C respectively. Maximum temperatures were centred in the sea while the minimum was near the slopes of Mt. Kilimanjaro.

The next charts figure 4.3 and figure 4.4 are also for the December-February season but for daytime values at 13 hours. The flow depicted is easterly from figure 4.3.

In the North-Eastern sector, wind blows in an easterly manner and reduces inland. As one moves down south, the wind speed increases at the coast. This is due to the dominance of the sea breeze formed by temperature gradients between the land and the sea. On the contrary, the topography on the eastern slopes of Mt. Kenya seem to have negative impact during the day-time. The large scale flow which is dominantly north-easterly at this time of the year seems to have been overcome by the effects of the sea breeze as given by figure 4.4. The temperature variation is from a maximum of 31°C in the sea to about 29°C inland. This therefore determines the overall characteristics of the local winds.

4.3 March-May and September-November seasons.

The second period considered was from the long rains and short rains seasons, when the sun is overhead on the equator. The mean flow during these seasons as given by Findlater (1968), in figures

4.9 and 4.10 is basically on-shore easterlies. Figure 4.6 gives the wind patterns during the night at 23 hours. It can be seen that in the North-East, the wind blows in an easterly manner from the sea. The wind speed decreases in intensity as it travels inland. From the North-West sector towards the south, wind decreases slightly towards the Mt. Kilimanjaro slopes. The northerly wind from the slopes of Mt. Kenya towards south is due to the downslope winds formed at night-time.

On the temperature chart figure 4.7, the temperature is highest at 26⁰c in the North-East sector and decreases inland. The land breeze effect is not obvious. The temperature gradient inland seems not to favour it. In this case, the behaviour of the wind field could be closely associated with the convergence zone being near the equator which is close to the study area.

The eastern slopes of Mt. Kenya seem to have an effect on the direction of wind during the night-time. It should be stressed that this is due to the low wind speed exhibited at night-time. The influence of the synoptic scale winds dominated over most areas. The synoptic scale wind speed was slightly higher than the generated flow.

In conclusion, it is noted that the mean flow is close to the generated flow and only differs in

WIND VELOCITY FIELD KEY
23:00HRS

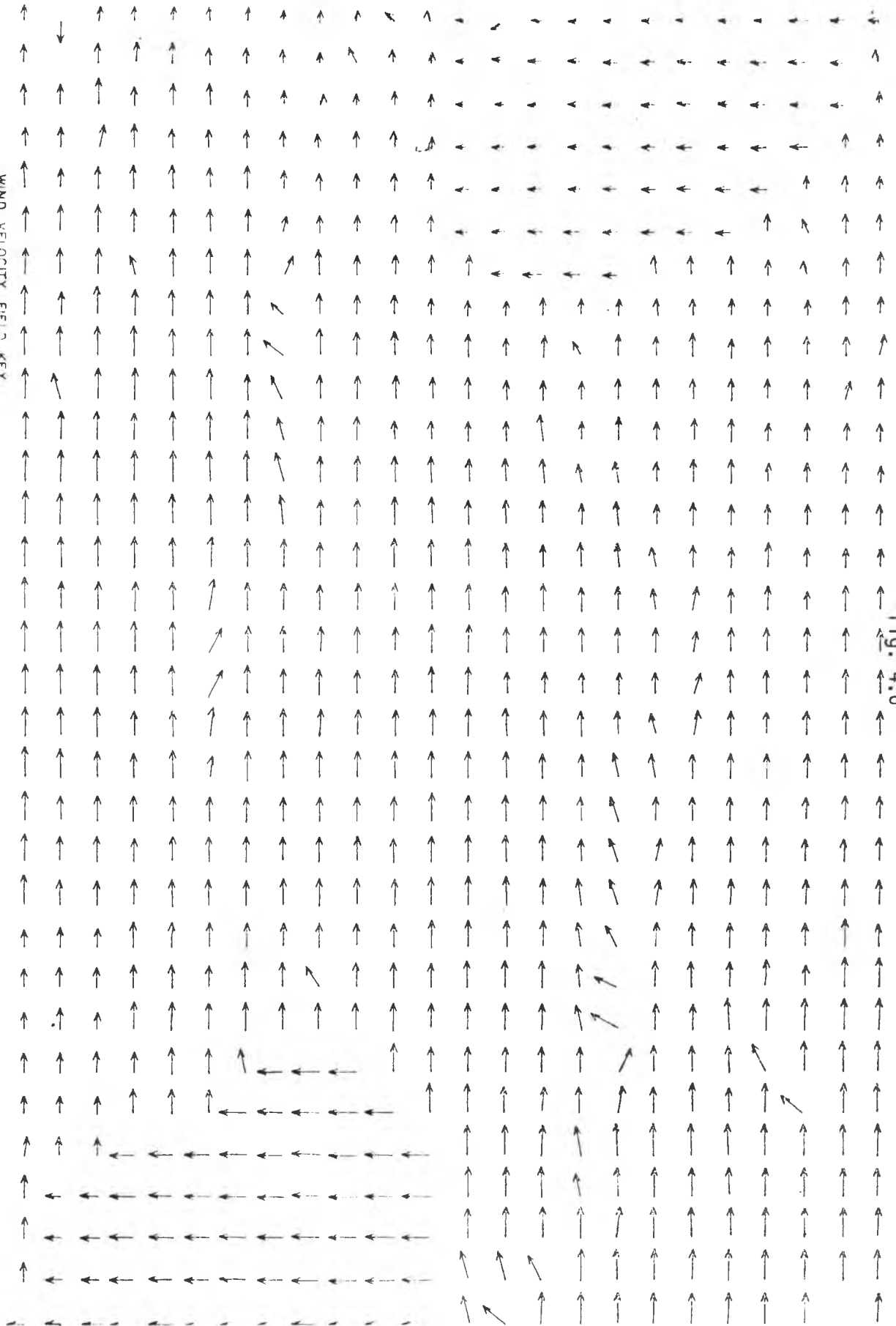
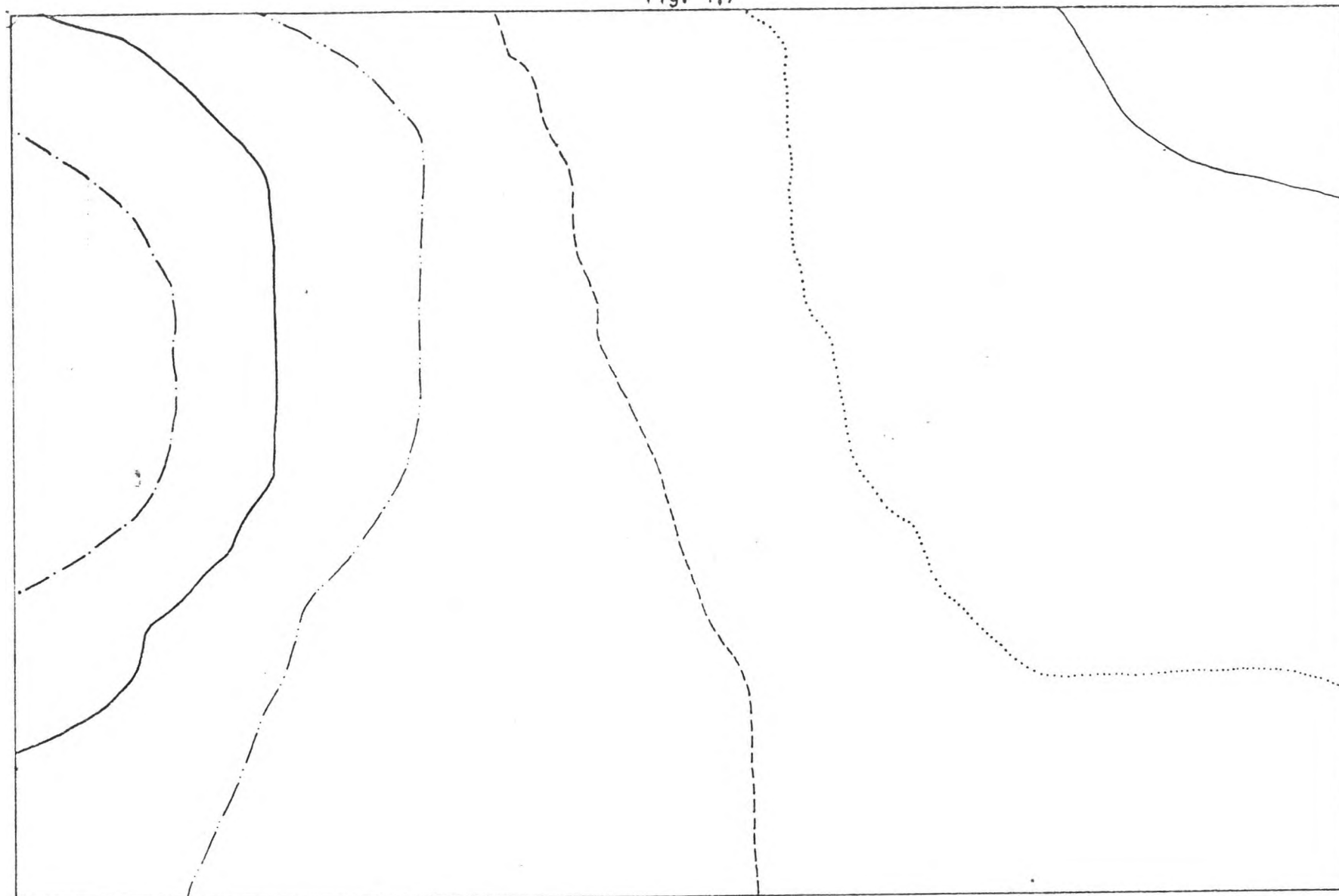


Fig. 4.6

fig. 4.7



TEMPERATURE KEY AT 2300HRS

20°C	— · — · — ·	22°C	— · — · — ·	24°C
21°C	—————	23°C	— · — · — ·	26°C	—————

WIND VELOCITY FIELD KEY
1300 HRS

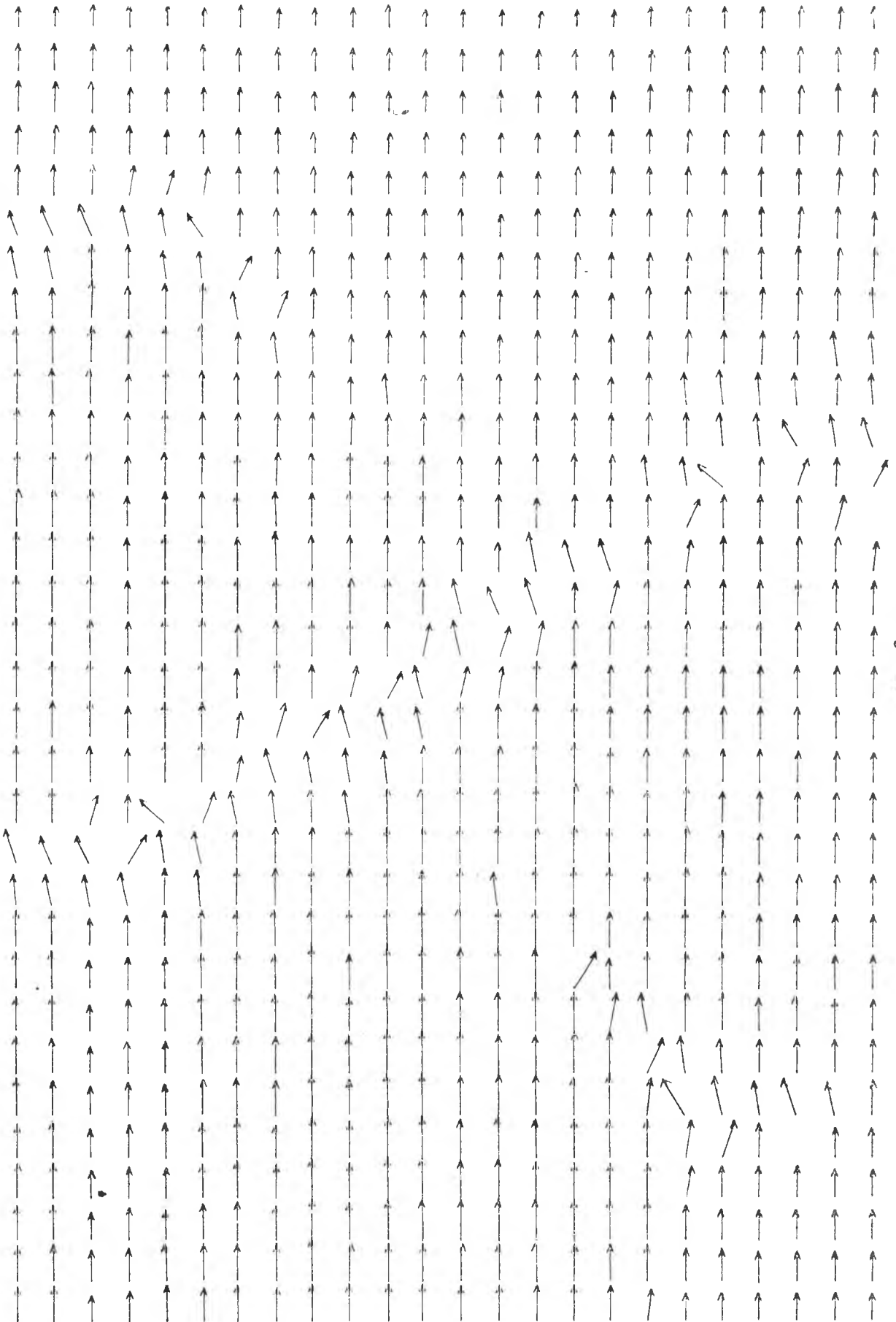


fig. 4.8

APRIL

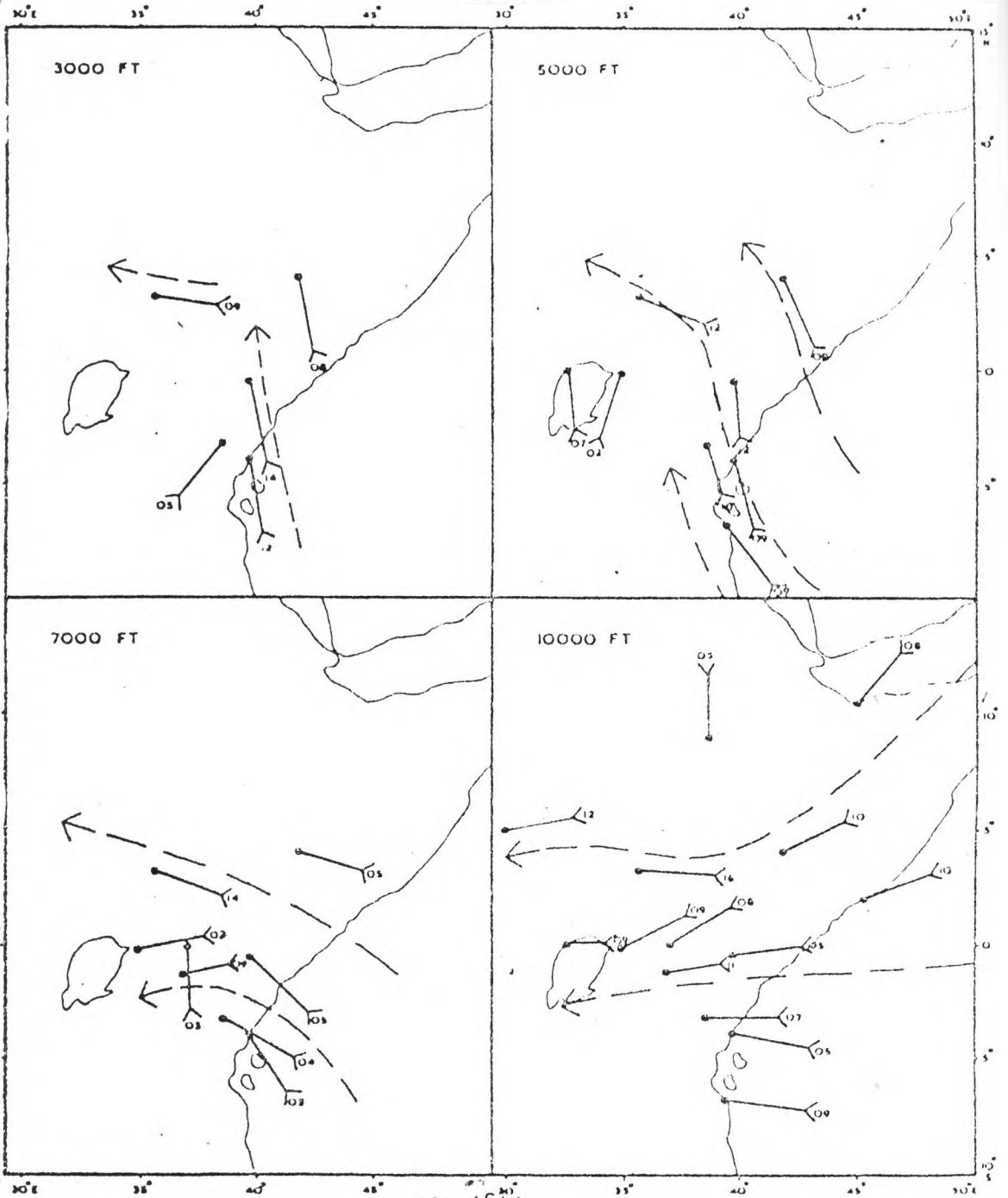
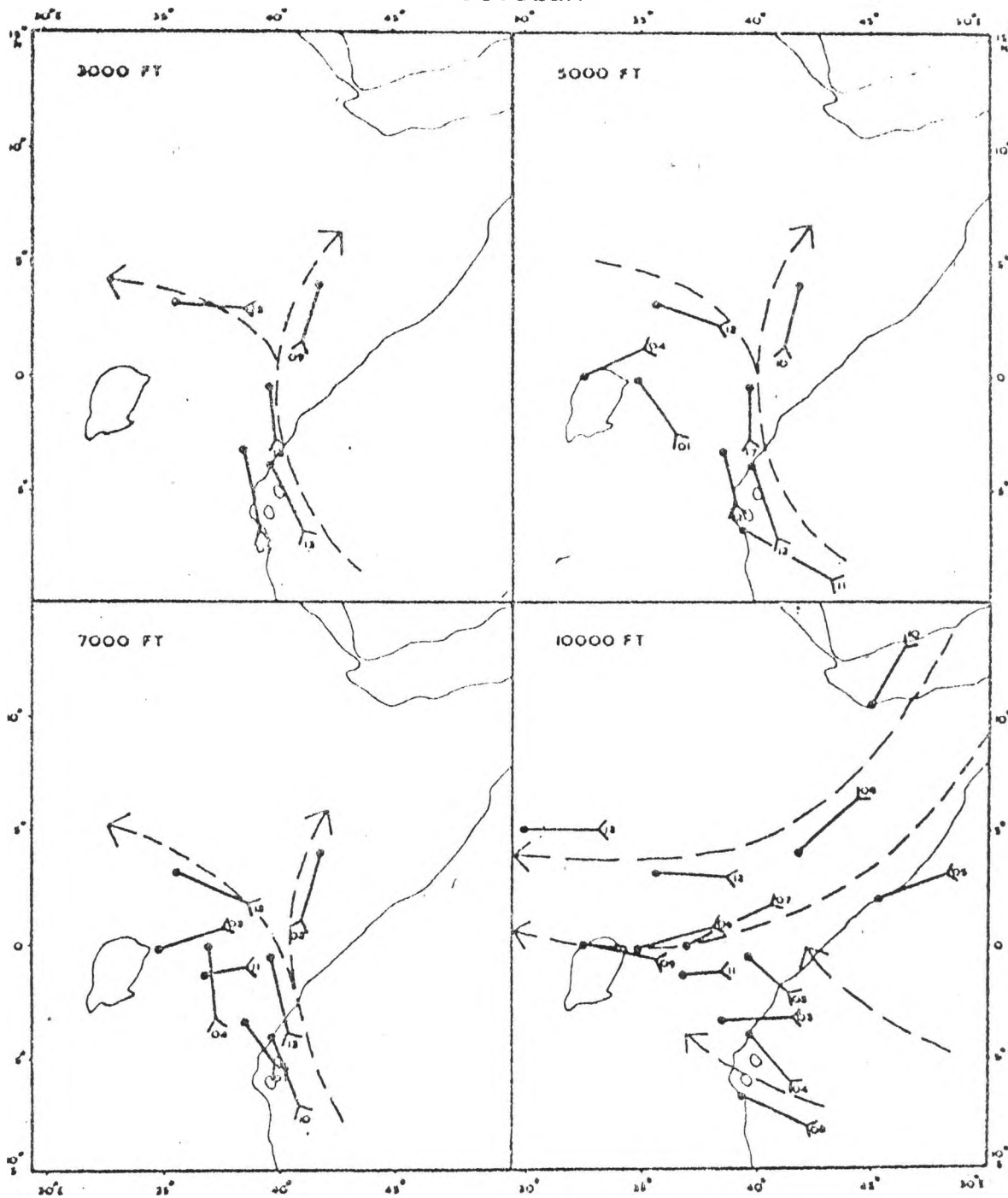


Fig. 4.9

fig. 4.10

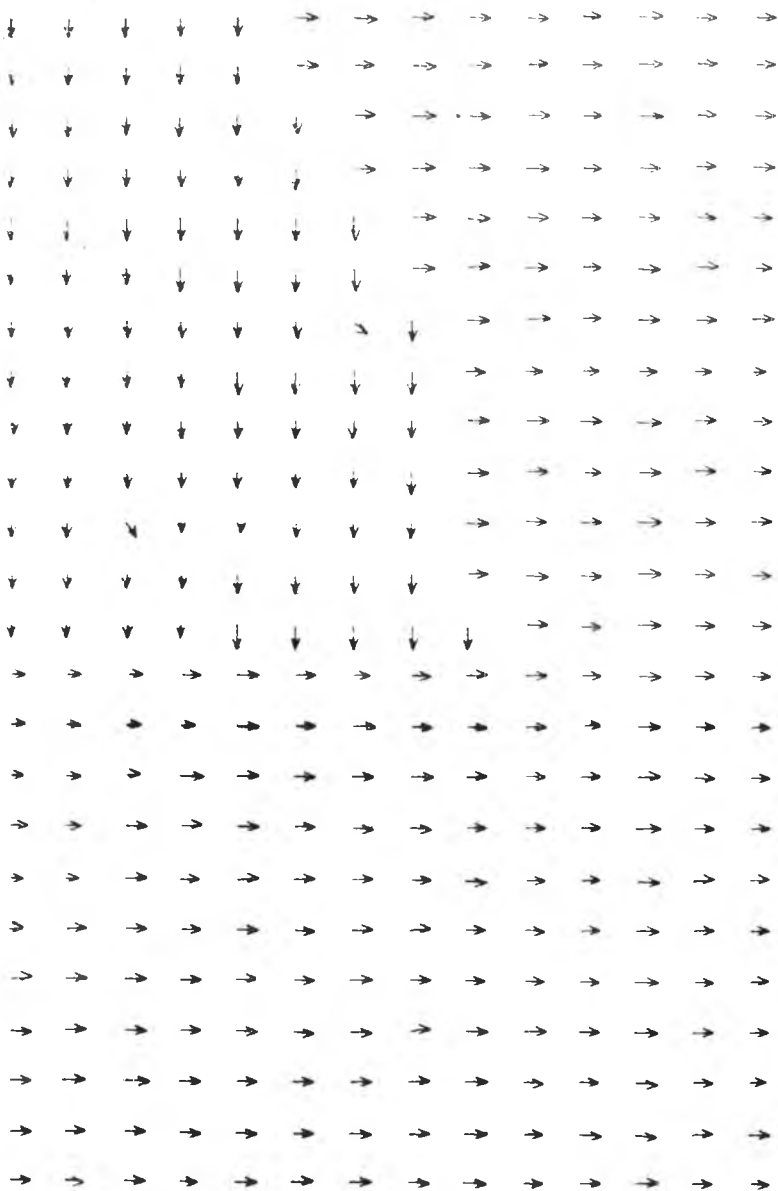
OCTOBER



magnitude. It is also noted that temperature patterns do not play a big role in determining the flow. Other studies by Ogallo and Anyamba (1986) observed that the wind characteristics change significantly during the wet and dry years. Wet conditions along coastal areas have been associated with stronger easterlies while weaker easterlies dominate during dry years. This year was a dry one.

4.4 June-August Season

The mean flow during this season is south easterlies (figure 4.15). It can be observed from our night-time chart (figure 4.11) that over the North-Eastern sector extreme winds blow in a northerly manner for about 40km and then suddenly changes to a westerly flow. The northerly wind could have been formed due to the katabatic flow of the eastern slopes of Mt. Kenya. This chart depicts weak winds inland of the study area and yet around Mombasa, winds are quite high blowing in a southerly direction. This could be due to sea surface temperature gradients which could not be examined due to data limitation. The wind pattern is similar to the December-February season (figure 4.1) for the night-time. The day-time wind pattern (figure 4.13) also shows the same similarity in the flow directions with the December-February season. The only difference is in the magnitudes, of which, the June-August season exhibits highest



WIND VELOCITY FIELD KEY
2300HRS

fig. 4.11

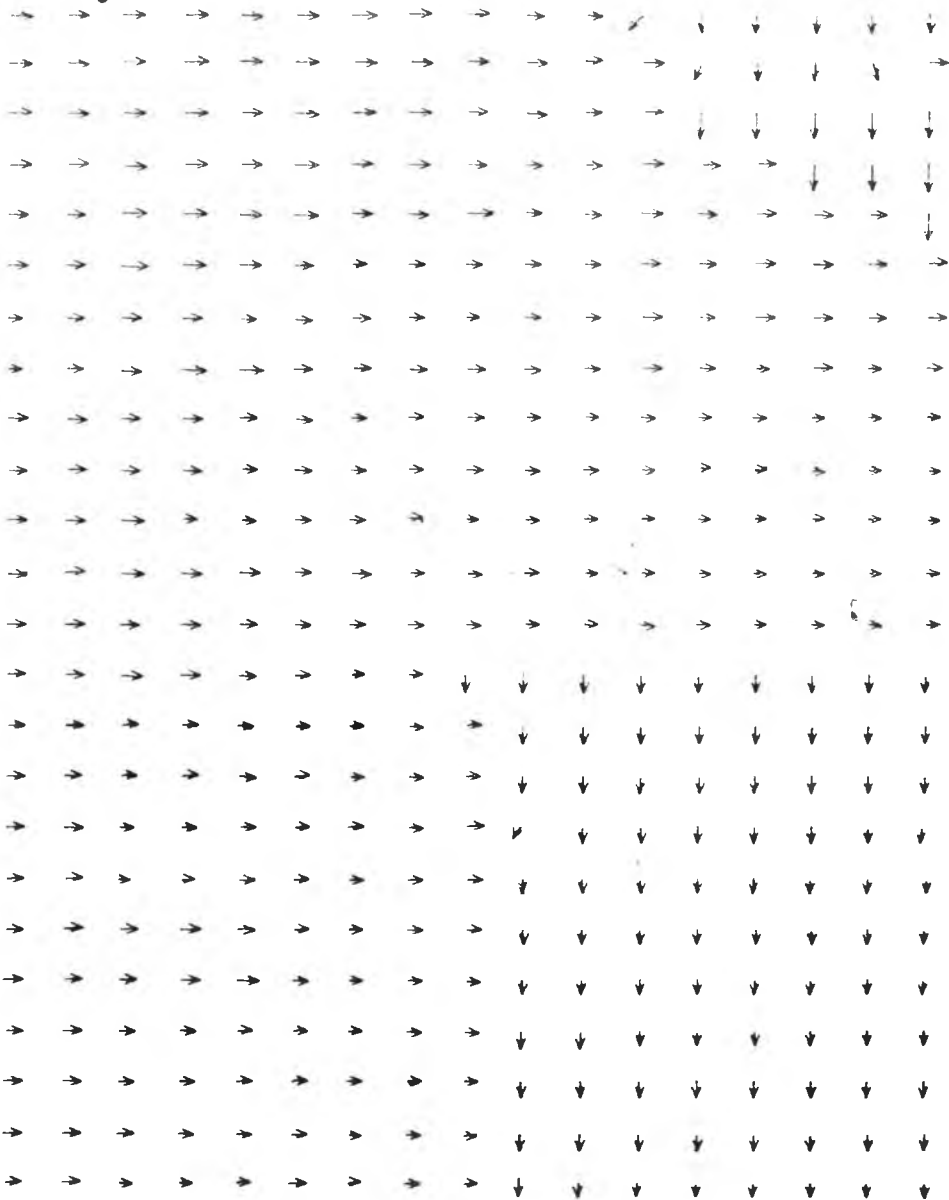


fig. 4.12



TEMPERATURE KEY AT 23:00 HRS

20°C ————
21°C ————

22°C ————
23°C ————

24°C
26°C ————

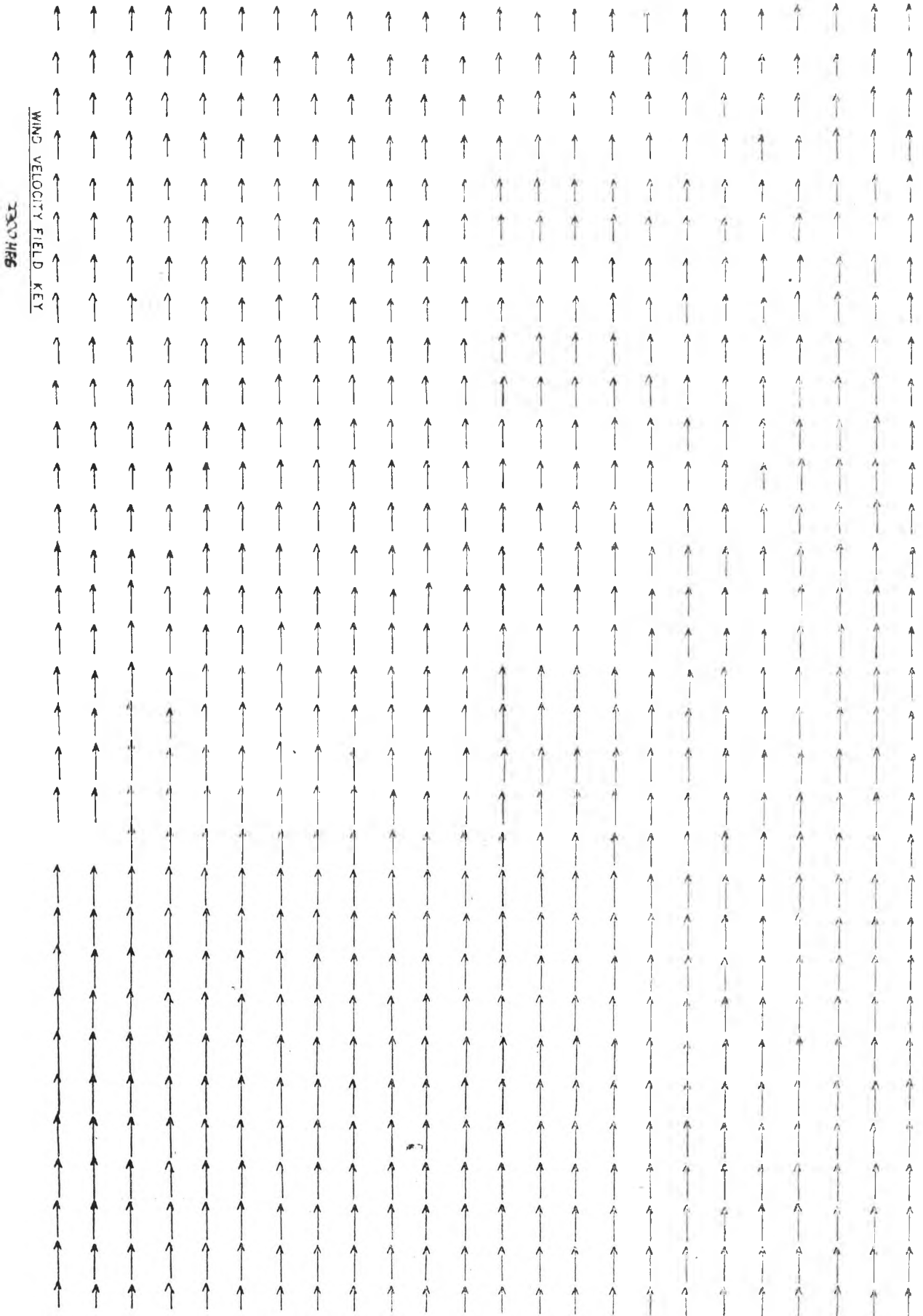
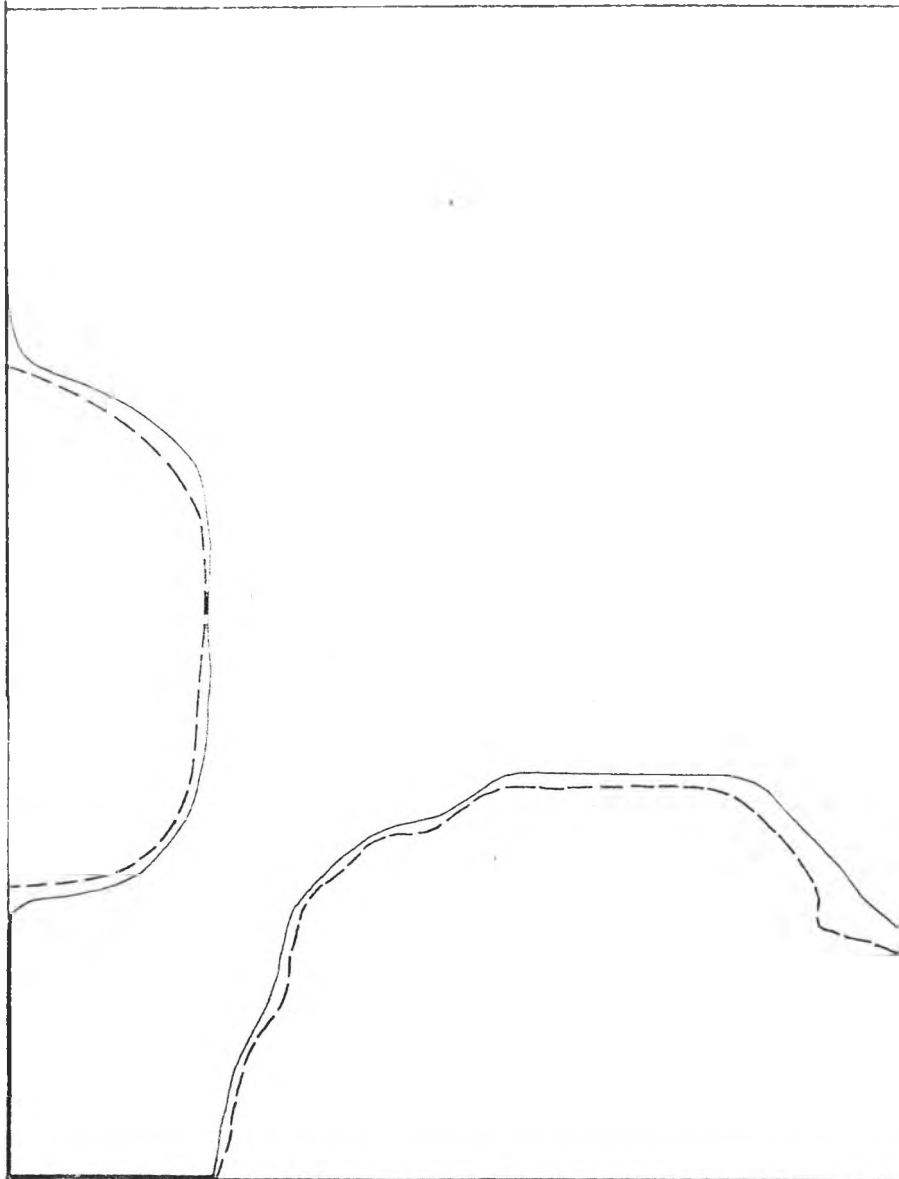


Fig. 4.13

- 5/ -



TEMPERATURE KEY AT 13 00 HRS

29°C ———
30°C ———

fig. 4.14

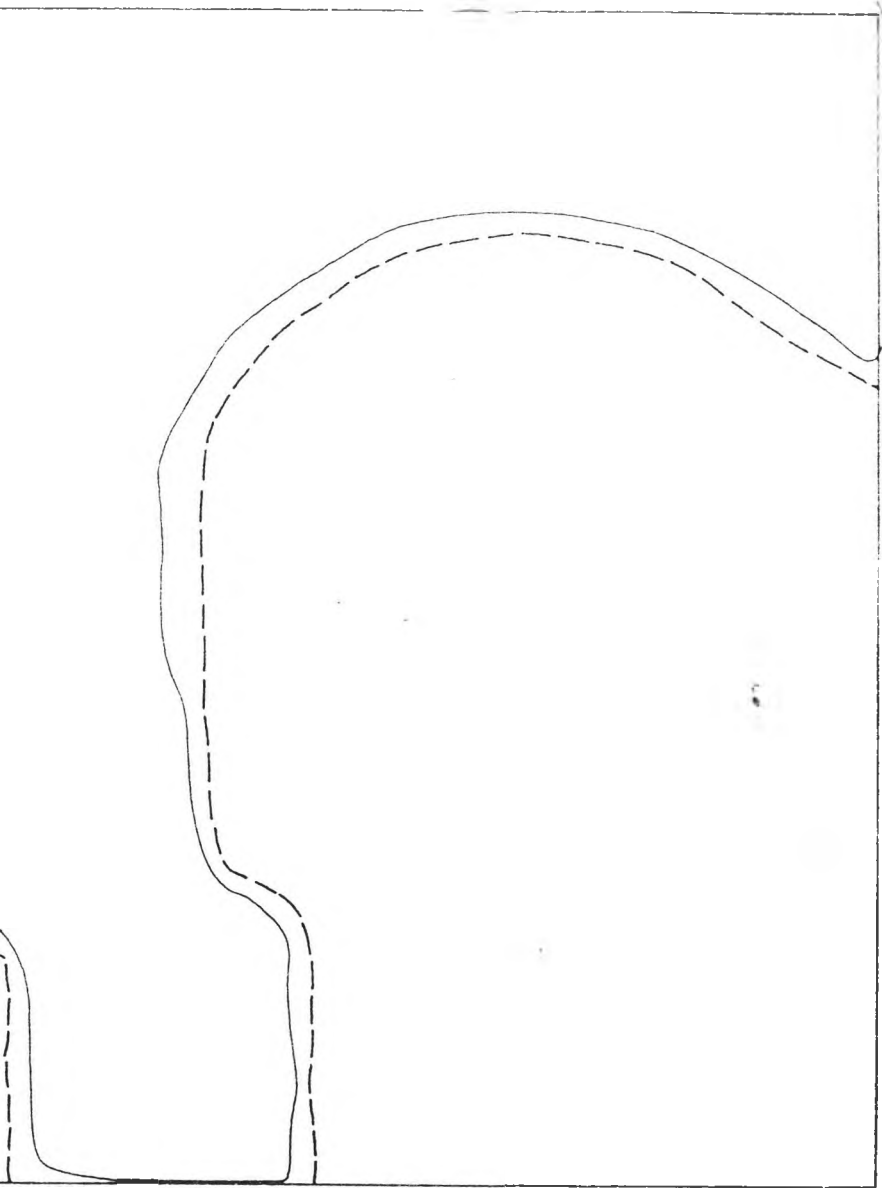
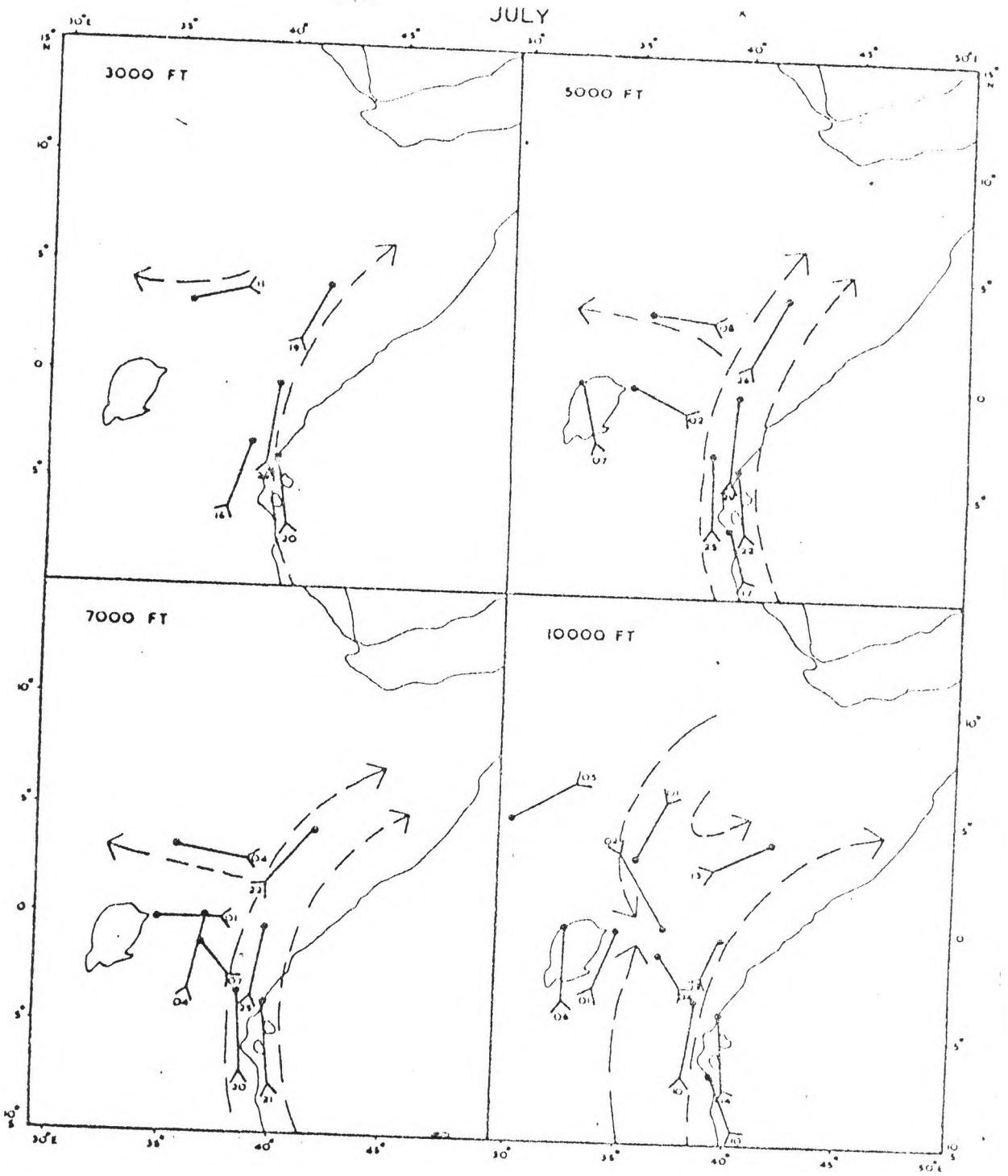


fig. 4.15



wind speeds and lowest wind speeds inland of the study area. In effect, there is higher variation of the wind speed in this season. This could be due to the combined effect of the synoptic scale flow and the sea breeze.

The night-time temperature chart (figure 4.12) depicted features that were similar to those observed during the night-time in the December-February season. The sea was much warmer than the land in both seasons but the temperatures in the June-August season were lower than the December-February season. The higher temperature variation exhibited in the June-August favours the effects of land-sea breeze circulations.

From our results we conclude that the method employed was capable of simulating reasonable diurnal as well as seasonal wind characteristics for the four standard seasons. It produces results that are dependable and which may be used in the initialization process for hydrodynamic solutions.

CHAPTER 5

SUMMARY AND CONCLUSION

The study was to apply a two-dimensional objective analysis to a region near the equator based on the surface layer of the atmospheric boundary layer. A vector field of wind velocity and a scalar field of temperature were interpolated in the horizontal. The model provided an initial field by filling a computational domain of 320km by 240km divided into grids of 10km by 10km over an East-coast area of Kenya.

The results indicated that the scheme used was capable of reasonably representing the seasonal and diurnal wind and temperature patterns. The results for one season were however not close to the mean seasonal expectations. This could be due to the fact that the mean seasonal flow is computed over long period observations, while the study observations were for only one year.

The magnitude of the wind speed that was computed in this study, compares well with those observed by Findlater (1968).

The model did not incorporate terrain features but this assumption does not hinder their effect on the wind flow as was seen in the study. A suggestion for further study would be towards the development of an interpolation technique or otherwise which can be

more accurately applied in the equatorial zones with treatment of the separate wet, dry and normal rainfall characteristics.

REFERENCES

1. Atkinson, G and Sadler, J.C., 1970. Mean cloudness and gradient level wind charts over the tropics, USAF AWS Tech. Reph. No. 21.
2. Bhumralkar, C.M.R.L. Mancuso, F.L. Ludwig and D.S. Renne 1980: A practical and economic method for estimation wind characteristics at potential wind energy conversion sites, Solar Energy, 25, 55-65.
3. Boone D, and G. Samuelson, 1977: Computer mapping of air equality. J. Environ. Eng. Div. Proc. ASCE, 103, EE6, 969-979.
4. Businger, J.A., J.C. Wyngaard, Y. Izumi and E.F. Bradley, 19 Flux profile relationships in the atmospheric surface layer. J. Atmos. Sci., 28, 181 - 189.
5. Byers, H.R., 1974: General Meteorology, Mcgraw-Hill Company.
6. Carbon, J.M., 1965: Shelterbelts and Wind breaks, G B Bowering Press Plymouth.
7. Chorlton, F., 1967: Textbook of Fluid Dynamics, D. Van Nostrand Company.
8. Cressman, G.P., 1959: An Operational Objective Analysis System. Mon. Wea. Rev., 87, 367 - 374.

9. Daubenmire, R.F., 1974: Plants and Environment, Wiley Eastern Private Limited, New Delhi.
10. Davis C.G., Bunker S.S., and Mutschlecner J.P.: 1984: Atmospheric transport models for Complex Terrain. Journal of Climate and Applied Meteorol., 23, 2, 235-2.
11. Dartt, D.G. 1972: Automated streamline analysis utilizing optimum interpolation. J. Appl. Meteorol., 11, 901 - 908.
12. Dickerson, M.H., 1973. A mass-consistent wind Field model for the San Francisco Bay area. UCRL-74265, Lawrence Livermore Laboratory, Calif.
13. E. Aubert de la rue, 1955: Man and the Winds, Hutchnson's Scientific and Technical publications, Stratford place London.
14. Endlich, R.M., and R.L. Mancuso, 1968: Objective analysis of Environmental conditions associated with severe Thunderstorms and Tornadoes. Mon. Wea. Rev. 96, 3, 342-39.
15. Endlich R.M., F.L. Ludwig, C.M. Bhumralkar and M.A. Esrogo 1982: A Diagnostic Model for Estimating Winds at potential sites for Wind Turbines. Journal of Applied Meteorol. 21, 1441-1454.
16. Fritsch, J.M., 1971: Objective analysis of a two-dimensional data field by the cubic spline technique. Mon. Wea. Rev. 99, 379-386.

17. Findlater, J. 1968: The month to month variation of winds at low levels over eastern Africa. EAMD Tech. memo No. 12, 27 pp.
18. Gandin, L.S., 1965: Objective analysis of Meteorological Fields. Israel Program for Scientific Translations, Jerusalem, 242 pp.
19. Garrett, J.A., 1983: Drainage flow prediction with a one-dimensional Model including Canopy Soil and Radiation Parameterization. Journal of climate and applied Meteorol. 22, 79-91.
20. Garrett J.A., and S.G. Frank III, 1984: Two-dimensional simulation of drainage winds and diffusion compared to observations. Journal of climate and applied Meteorol. 23.
21. Glahn H.R., 1981, Comments on "A comparison of interpolation methods for sparse data: Application to wind and concentration fields. Journal of applied meteorology, 20, 88-91.
22. Gilchrist B. and Cressman, G.P., 1954: An experiment in objective analysis, Tellus, A quarterly journal of Geophysics, 6, 4, 309-318.
23. Goodin W.R., G.J. McRae and J.H. Seinfeld, 1979: A comparison of interpolation methods for sparse data: Application to wind and concentration fields. Journal of applied

Meteorol., 18, 761-771.

24. Haltiner, G.J., 1971: Numerical Weather prediction. John Wiley and Sons, Inc.
25. Holton, J.R., 1972. An Introduction to dynamic Meteorology. Academic Press (New York and London), Inc.
26. Hovland D, D. Dartt and K. Gage, 1977: An Objective analysis technique for the regional air pollution study, Part I, EPA, Research Triangle Park, N.C., 44 pp. [NTIS PB 266255].
27. Kavishe M.M., 1983: M.Sc. Thesis. Three-dimensional Mean wind flow and thickness patterns over Africa.
28. Kidson, J.W., Vincent, D.G. and Newel, R.E., 1969: Observational studies of the general circulation of the tropics. Long term mean values. Q.J. Roy. Met. Soc., 95, 258-287.
29. Lalas, D.P. 1983: Modelling of the wind flow over crete for wind energy estimation, EVROMECH-173, - September 1983. Delphin, Greece.
30. Lalas, D.P. 1985: Wind energy estimation and siting in complex terrain. Int. J. Solar Solar Energy, 3, 43-71.
31. Lalas, D.P., 1986: Brief outline of boundary layer theory, internal report, ICTP, 21st April - 16th May.

32. Lawson, C.L., 1977: Software for c' surface interpolation Mathematical Software, vol. 3, J.R. Rice, Ed., Academic Pre. 161-194.
33. Lee, R.L., W.S. Kan and S.K. Kao, 1982: A Statistical model for surface pollutant concentration prediction in complex terrain, 12th Int. Technical meeting on Air Pollution Modelling and its Application, Palo auto; California.
34. Liu, M.K. and M.A. Yocke, 1980: Siting of wind turbine generators in complex terrain. J. Energy, 4, 10-16.
35. Mahrer, Y and R.A. Pielke, 1975: A numerical study of the air flow over mountains using the 2-D version of the UVMM. J. Atmos. Sci., 32, 2144-2156.
36. McCracken, M.C. and G.D. Sauter, Eds., 1975: Development of an air pollution Model for the San Fransisco Bay Area vol. 2, Appendices. Lawrence Livermore Laboratory, UCRL-51920, 229-230 |NTIS UCRL-51920|.
37. McLain, D.H., 1974: Drawing contours from arbitrary data points. Comput. J., 19, 318-324 , 1976: Two dimensional interpolation from randian data comput. J., 19, 178-181.

38. Mellor, G.L. and T. Yamada, 1982: Development of a turbulence closure scheme for geophysical fluid models. *Rev. Geophys. Space Phys.* 20, 851-875.
39. Ogallo L.J. and E.K. Anyamba, 1986: Draughts of tropical central and eastern Africa July-November 1983, northern spring of 1983-84: Reprints from WMO/TD No. 87, pp 67-62.
40. Panofsky, H.A., 1949: Objective Weather-map analysis *J. Meteor.*, 6, 386-392.
41. Pao, Richard H.F., 1964: *Fluid Mechanics.* John Wiley and Sons.
42. Patnaik, P.C., 1979: A preliminary users guide for the DIGMET mesoscale meteorology code, SAI Report SAI-75 LJ., RLQ/2440-77-9, July 1979, San Diego, California.
43. Pearson, R.A. and O'Connor., S., 1977: A numerical dynamical instability. *Mon. Wea. Rev.*, 105, 301-316.
44. Prandtl L., 1952: *Essentials of fluid dynamics* Blackie and Sons Ltd.
45. Putnam P.C., 1948: *Power from the Wind.* Van Nostrand Reinhold Company, New York.

46. Sasaki, Y., 1958: An objective analysis based on the variational method. Journal of Met.-Soc. of Japan, Sen. II, 36, 3, 77-88.
47. Sasaki Y., 1970: Some basic formations in numerical variational analysis. Mon. Wea. Rev. 98, 875-883.
48. Schaffer, J.T. and Charles A. Doswell III, 1979: On the interpolation of a vector field. Mon. Wea. Rev, 107, 4, 458-476.
49. Scorer, R.S., 1978: Environmental aerodynamics, Ellis Horwood Ltd. John Wiley and Sons.
50. Seaman, N.L. and R.A. Anthes, 1981: A mesoscale semi-implicit numerical model. Quart. J. Roy. Meteorol. Soc., 107, 167-190.
51. Sherman, C.A. 1978: A mass-consistent model for which fields over complex terrain J. Appl. Meteorol., 17, 312-319.
52. Shenfeld, L, and A.E. Boyer, 1974: The utilization of an urban air pollution model in air management. Paper presented at fifth meeting NATO/CCMS Expert Panel on Air Pollution Modelling, Roskilde, Denmark.
53. Shepard, D., 1968: A two-dimensional interpolation function for irregularly spaced data. Proc. 23rd ACM Nat. Conf., Las. Vegas, 517-524.

54. Thiessen, A.H. 1911: Precipitation averages for large areas. Mon. Wea. Rev., 39, 1082-1084.
55. Traci, R.M., G.T. Phillips. P.C. Patnaik and B.E. Freeman, 1977: Development of a wind energy site selection methodology U.S. Dept. of Energy Report RL0/2440-1 205 pp.
56. WMO Technical Note No. 575: Meteorological aspects of the utilization of wind as an energy source.
57. Wilkins, E.M., Sasaki, Y.K. Gerber, G.E. and Chaplin, W.H., Jr., 1976: Numerical Simulation of the lateral interactions between bouyant clouds. J. Atmos. Sci., 33, 1321-1329.